

# The Genomic Loci of Specific Human tRNA Genes Exhibit Ageing-Related DNA Hypermethylation

Richard J. Acton <sup>1</sup>, <sup>2</sup>, <sup>3</sup>, Wei Yuan <sup>4</sup>, <sup>5</sup>, Fei Gao <sup>6</sup>, Yudong Xia <sup>6</sup>, Emma Bourne <sup>7</sup>, Eva Wozniak <sup>7</sup>, Jordana Bell <sup>4</sup>, Karen Lillycrop <sup>3</sup>, Jun Wang <sup>6</sup>, Elaine Dennison <sup>2</sup>, Nicholas Harvey <sup>2</sup>, Charles A. Mein <sup>7</sup>, Tim D. Spector <sup>4</sup>, Pirro G. Hysi <sup>4</sup>, Cyrus Cooper <sup>2</sup>, Christopher G. Bell <sup>1</sup> \*

**1** William Harvey Research Institute, Barts & The London School of Medicine and Dentistry, Charterhouse Square, Queen Mary University of London, London, U.K.

**2** MRC Lifecourse Epidemiology Unit, University of Southampton, Southampton, U.K.

**3** Human Development and Health, Institute of Developmental Sciences, University of Southampton, Southampton, U.K.

**4** Department of Twin Research & Genetic Epidemiology, St Thomas Hospital, King's College London, London, U.K.

**5** Institute of Cancer Research, Sutton, U.K.

**6** BGI-Shenzhen, Shenzhen, China

**7** Barts & The London Genome Centre, Blizard Institute, Barts & The London School of Medicine and Dentistry, Queen Mary University of London, London, U.K.

\* Corresponding author:

## Abstract

The epigenome deteriorates with age, potentially impacting on ageing-related disease.

Here, we interrogate the DNA methylation state of the genomic loci of human tRNA. Whilst arising from only ~46kb (<0.002% genome), this information transfer machinery is the second most abundant cellular transcript. tRNAs also control metabolic processes known to affect ageing, through core translational and additional regulatory roles.

We identified a genomic enrichment for age-related DNA hypermethylation at tRNA loci. Analysis in 4,350 MeDIP-seq peripheral-blood DNA methylomes (16–82 years), classified 44 and 21 hypermethylating specific tRNAs at study- and genome-wide significance, respectively, contrasting with 0 hypomethylating. Validation and replication (450k array & independent targeted Bisulfite-sequencing) supported the hypermethylation of this functional unit. The strongest consistent signals, also independent of major cell-type change, occur in tRNA-iMet-CAT-1-4 and tRNA-Ser-AGA-2-6.

This study is the first comprehensive evaluation of the genomic DNA methylation state of human tRNA genes and reveals a discreet hypermethylation with advancing age.

## Introduction

Ageing is implicated as a risk factor in multiple chronic diseases [1]. Understanding how the ageing process leads to deteriorating biological function is now a major research focus, with hopes to increase the human ‘healthspan’ and ameliorate the extensive physical, social and economic costs of these ageing-related disorders [2]. Epigenetic processes, which influence or can inform us about cell-type specific gene expression, are altered with age and are, furthermore, one of the fundamental hallmarks of this progression [3,4].

DNA methylation (DNAm) is the most common epigenetic modification of DNA and age-associated changes in this mark in mammalian tissues have been recognised for decades [5]. In fact, these alterations in DNAm with age are extensive with thousands of loci across the genome affected. Many represent ‘drift’ arising from the imperfect maintenance of the epigenetic state [6]. However, specific genomic regions show distinct directional changes, with loss of DNA methylation in repetitive or transposable elements [7], as well as gains in certain promoters, including the targets of polycomb repressor complex [8] and bivalent domains [9]. These observations with the advent of high-throughput DNAm arrays also permitted the identification of individual CpG sites that exhibit consistent changes with age, enabling the construction of predictors of chronological age known as epigenetic or DNAm ‘clocks’ [10–13]. Additionally, it was observed that ‘acceleration’ of this DNAm-derived measure is a biomarker of ‘biological’ ageing due to associations with morbidity and mortality (Reviewed in [14] & [15]). In a previous investigation of ageing-related DNAm changes within common disease-associated GWAS regions, we identified hypermethylation of the specific transfer RNA gene, tRNA-iMet-CAT-1-4 [16]. The initiator methionine tRNA possesses certain unique properties, including its capacity to be rate limiting for translation [17], association with the translation initiation factor eIF2 [18], and ability to impact the expression of other tRNA genes [19].

tRNAs are evolutionarily ancient [20] and fundamental in the translation process for all domains of life. This translation machinery and the regulation of protein synthesis are controlled by conserved signalling pathways shown to be modifiable in longevity and ageing interventions [21]. Additionally, beyond their core role in the information flow from DNA to protein sequence, tRNAs can fragment into numerous tRNA-derived small RNAs (tsRNAs) [22] with signalling and regulatory functions [23–26].

When liberally considering the 610 loci annotated as tRNA genes, as well as tRNA pseudo genes, nuclear encoded mitochondrial tRNA genes and possibly some closely related repetitive sequences, these features (gtRNADB [27]) cover <46 kb (including introns) which represents <0.002% of the human genome [28]. Yet a subset of these genes produce the second most abundant RNA species next to ribosomal RNA [29] and are required for the production of all proteins. tRNA genes are transcribed by RNA polymerase III (polIII) [30] and

have internal type II polIII promoters [31]. DNAm is able to repress the expression of tRNA genes 46 experimentally [32] but may also represent co-ordination with the local repressive chromatin state [33]. 47 Transcription is also repressed by the highly conserved polIII specific transcription factor Maf1 [34,35], who's 48 activity is modulated by the Target of Rapamycin Kinase Complex 1 (TORC1) [36]. TORC1 is a highly 49 conserved hub for signals that modulate ageing [37]. 50

tRNAs as well as tsRNAs are integral to the regulation of protein synthesis and stress response, two processes 51 known to be major modulators of ageing. Metabolic processes are also recognised to modulate the age estimates 52 of DNAm clocks [38]. Partial inhibition of translation increases lifespan in multiple model organisms [39] and 53 PolIII inhibition increases longevity acting downstream of TORC1 [40]. Furthermore, certain tsRNAs circulating 54 in serum can be modulated by ageing and caloric restriction [41]. 55

We directly investigated ageing-related changes in the epigenetic DNA methylation state of the entire tRNA 56 gene set, facilitated by the availability of a large-scale MeDIP-seq dataset. Arrays poorly cover this portion of 57 genome, with even the latest EPIC (850k) arrays only covering <15% of the tRNA genes, with robust probes, and 58 in total only ~4.7% of all the tRNA gene CpGs [42]. tRNA genes sit at the heart not only of the core biological 59 process of translation but at a nexus of signalling networks operating in several different paradigms, from small 60 RNA signalling to large scale chromatin organisation [43]. In summary, tRNA biology, protein synthesis, nutrient 61 sensing, stress response and ageing are all intimately interlinked. In this study, we have identified tRNA gene 62 DNA hypermethylation and independently replicated this newly described ageing-related observation. 63

## Results

64

### DNA Methylation of Specific tRNA Gene Loci Changes with Age

65

Due to tRNAs critical role in translation and evidence of their modulation in ageing and longevity-related pathways, we interrogated these genes for evidence of ageing-related epigenetic changes. Our discovery set was a large-scale peripheral blood-derived DNA methylome dataset comprising of 4350 samples. This sequencing-based dataset had been generated by Methylated DNA Immunoprecipitation (MeDIP-seq) [44], which relies on the enrichment of methylated fragments of 200-500 bp to give a regional DNAm assessment (500 bp semi-overlapping windows, see Methods). There are 416 high confidence tRNA genes in the human genome, we initially examined an expanded set of 610 tRNA-like features identified by tRNAscan including pseudogenes, possible repetitive elements, and nuclear encoded mitochondrial tRNAs [27,45]. Of these 492 were autosomal and did not reside in blacklisted regions of the genome [46]. Due to the small size of these tRNAs (60-86bp, median 73bp, excluding introns which are present in ~30 tRNAs with sizes from 10-99bp, median 19bp), this fragment-based method enabled a robust examination of the epigenetic state of these highly similar sequences. This was supported by a mappability assessment. The median mappability score density for all tRNA genes was 0.90 for 50mers when considering tRNA genes  $\pm 500\text{bp}$  reflecting the regional nature of the MeDIP-seq assay. In contrast the 50mer mappability density is 0.68 for tRNA genes alone, which would be representative of the mappability of reads generated using a technique such as whole-genome bisulfite sequencing (see Figures S1 & S2).

We identified 21 genome-wide significant and 44 study-wide significant results ( $p < 4.34 \times 10^{-9}$  and  $8.36 \times 10^{-5}$ , respectively, via linear regression ( $n=4350$ , see Methods). Study-wide significance was calculated conservatively with the Bonferroni method for all 598 autosomal tRNAs and closely related features. There was a strong directional trend with all results at both significance levels being due to increases in DNA methylation. Age-related changes in cell type proportion are strong in heterogeneous peripheral blood, and include a myeloid skew, loss of naive T cells and increases in senescent cells [47]. A subset of 3 genome-wide and 16 study-wide significant hypermethylation results remained significant even after correcting for potential cell-type changes by including lymphocytes, monocytes, neutrophils and eosinophil cell count data ( $n=3001$ , Listed in Figure 1, see Figure S3). Going forward we refer to these cell-type corrected sets of 3 and 16 tRNA genes as the genome-wide and study-wide significant tRNA genes respectively.

tRNA	Window	MeDIP		450k Array		Targeted BiS-seq	
		Slope	p-value	Slope	p-value	Slope	p-value
tRNA-Gln-CTG-7-1	Chr1:147,800,750-147,801,250	0.84	2.60e-05				
	Chr2:131,094,500-131,095,000	1.11	4.64e-09				
tRNA-Glu-TTC-1-1	Chr2:131,094,250-131,094,750	1.00	1.12e-07				
	Chr2:131,094,750-131,095,250	1.00	3.28e-07				
tRNA-His-GTG-1-2	Chr1:146,544,500-146,545,000	0.92	1.38e-06				
tRNA-His-GTG-2-1	Chr1:149,155,750-149,156,250	1.05	2.98e-08				
	Chr1:149,155,500-149,156,000	0.83	1.37e-05				
tRNA-Ile-AAT-10-1	Chr6: 27,251,500- 27,252,000	1.07	1.45e-08			1.30	1.22e-03
	Chr6: 27,251,750- 27,252,250	0.90	1.86e-06			1.30	1.22e-03
tRNA-Ile-AAT-4-1	Chr17: 8,130,000- 8,130,500	1.19	2.98e-10	19.63	8.92e-06	-0.74	6.88e-04
	Chr17: 8,130,250- 8,130,750	0.77	3.99e-05	19.63	8.92e-06	-0.74	6.88e-04
tRNA-Ile-TAT-2-2	Chr6: 26,987,750- 26,988,250	0.97	7.25e-07	4.16	1.17e-02	-0.60	3.84e-01
tRNA-iMet-CAT-1-4	Chr6: 26,330,500- 26,331,000	1.28	2.83e-11	13.01	6.07e-06	4.54	9.35e-04
	Chr6: 26,330,250- 26,330,750	1.13	2.89e-09	13.01	6.07e-06	4.54	9.35e-04
tRNA-Leu-TAG-2-1	Chr14: 21,093,250- 21,093,750	1.04	9.38e-08			2.49	8.77e-03
	Chr14: 21,093,500- 21,094,000	0.94	8.50e-07			2.49	8.77e-03
tRNA-Pro-AGG-2-2	Chr6: 26,555,500- 26,556,000	1.04	3.97e-08				
	Chr6: 26,555,250- 26,555,750	1.01	9.58e-08				
tRNA-Ser-ACT-1-1	Chr6: 27,261,250- 27,261,750	0.97	3.53e-07			0.66	1.45e-01
tRNA-Ser-AGA-2-6	Chr17: 8,129,750- 8,130,250	1.21	1.16e-10	20.87	6.72e-05	0.62	4.28e-02
	Chr17: 8,130,000- 8,130,500	1.19	3.03e-10	20.87	6.72e-05	0.62	4.28e-02
tRNA-Ser-TGA-2-1	Chr6: 27,513,000- 27,513,500	0.90	3.58e-06	87.21	1.38e-04	-0.25	5.74e-01
tRNA-Val-AAC-1-2	Chr5:180,590,750-180,591,250	0.91	3.28e-06				
tRNA-Val-AAC-4-1	Chr6: 27,648,500- 27,649,000	1.07	1.25e-08	40.06	9.90e-03		
	Chr6: 27,648,750- 27,649,250	0.95	4.31e-07	40.06	9.90e-03		
tRNA-Val-CAC-2-1	Chr6: 27,247,750- 27,248,250	0.85	2.33e-05	59.16	5.05e-06		

**Fig 1.** Ageing-related DNA methylation changes in tRNA loci (16 Study-wide significant after blood cell-type correction,  $p < 8.36 \times 10^{-5}$ ). Columns left to right: tRNA gene; Genomic location of MeDIP-seq significant window (hg19); MeDIP results slope (arbitrary units) and p-value; 450k Array results slope (beta) and p-value (Blood-cell corrected and combined for all probes overlapping tRNA); Targeted Bisulphite-sequencing (BiS-seq) slope (beta) and p value (combined all CpGs in targeted region, see Methods) For slope: Orange = hypermethylation and Blue = hypomethylation with age. For p-values: Colour gradient high significance = dark blue to low significance = yellow, scaled relative to column. Blank grey cells indicate unavailable data.

Due to the related nature of these twin samples, we also analysed these data in two subsets of  $n = 1198$  & 1206 by selecting one twin from each pair into the separate sets. This analysis also included correction for Blood Cell counts. Even in these smaller sets, 5 and 7 tRNA genes, respectively, reached study-wide significance. In these sets 5/5 and 6/7 of these were present in 16 study-wide significant tRNA genes.

Furthermore, we examined a subset of samples with longitudinal data ( $n=658$  methylomes from 329 individuals, median age difference 7.6 yrs). At the nominal significance threshold ( $p < 0.05$ ) this yielded a split of 41 hypermethylating tRNA genes and 22 hypomethylating tRNA genes. Of these hypermethylated tRNAs, 2

are in the previously identified genome-wide significant set of 3 (with tRNA-iMet-CAT-1-4 ranked 3rd by p-value) 98  
and 9 are in the study-wide significant set of 16. Full results for each age model are provided in Supplementary 99  
File S1 100

## tRNA Genes are Enriched for Age Related DNA Hypermethylation 101

Whilst ageing changes are pervasive throughout the DNA methylome, we identified a strong enrichment for this 102  
to occur within the tRNA genes (Fisher's Exact Test  $p = 1.05 \times 10^{-27}$ ) (see Figure 2 b). This is still significant if 103  
the 6 of the study-wide significant 16 tRNAs that have any overlap with polycomb or bivalent regions are 104  
excluded ( $p = 4.66 \times 10^{-15}$ ) 105

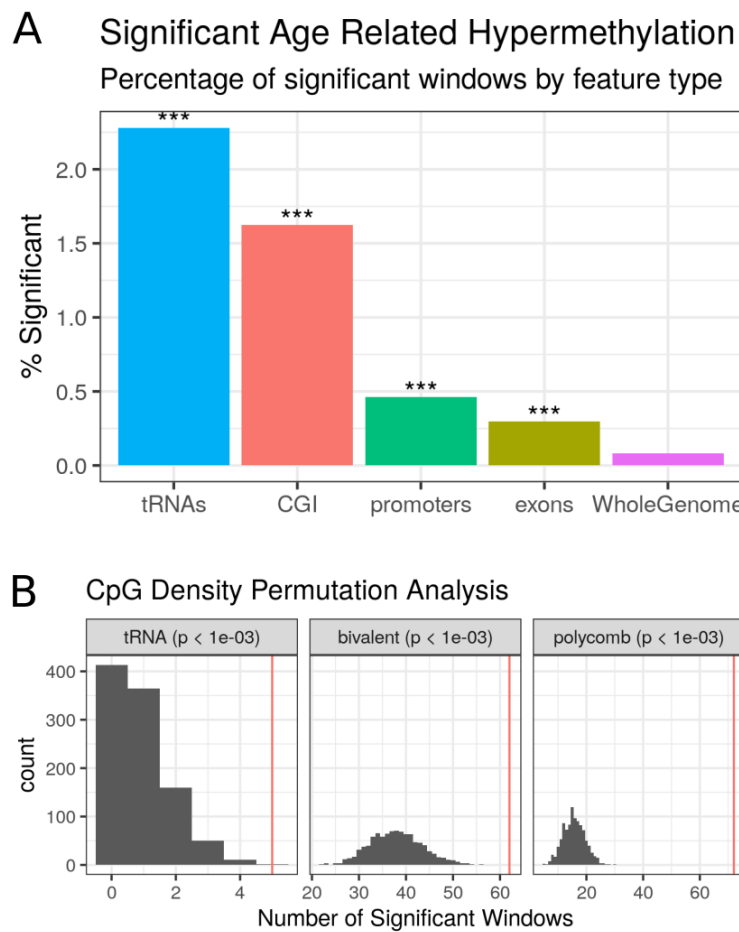


**Fig 2. A)** tRNA genes are enriched for age-related hypermethylation compared to the genomic background, (Fisher's Exact Test  $p < 1.05 \times 10^{-27}$ ,  $n = 3001$ ). **B)** tRNA genes show more significant hypermethylated loci than CpG Density matched permutations. Each permutation represented a random set of windows matching the CpG density of the functional unit (tRNA gene loci, bivalent domains, and polycomb group target promoters). These are subsequently assessed for significant age-related DNAm changes (see Methods). The red line is the observed number of significant loci.

CpG density itself is known to have a clear impact on the potential for variability of the DNA methylome as  
106 well as ageing-related changes [48,49]. To assess whether this hypermethylation finding was being merely driven  
107 by the inherent CpG density of the tRNA genes, we performed a CpG density matched permutation analysis  
108 (1,000X, see Methods). This supported the specific nature of these age-related DNAm changes within the  
109 functional tRNA genes (Empirical p-value <  $1.0 \times 10^{-3}$ , Figure 2 a). As a point of comparison for this genomic  
110 functional unit, we also performed the same permutations for the known age-related changes in the promoters of  
111 genes that are polycomb group targets [8] and those with a bivalent chromatin state [9]. We were able to  
112 reproduce the enrichment of the polycomb group targets and bivalent regions (Empirical p-value <  $1.0 \times 10^{-3}$ ) in  
113 our dataset.  
114

tRNA-iMet-CAT-1-4 (Figure 3a) is located in the largest tRNA gene cluster in the human genome at  
115 chr6p22.2-1. This cluster contains 157 tRNA genes spanning the 2.67Mb from tRNA-iMet-CAT-1-2 to  
116 tRNA-Leu-AAG-3-1, and also hosts a histone gene microcluster. tRNA-Ile-AAT-4-1 and tRNA-Ser-AGA-2-6 are  
117 neighbours and are located on chromosome 17 (Figure 3b). Notably tRNA-Ile-AAT-4-1 and tRNA-Ser-AGA-2-6  
118 have a third close neighbour tRNA-Thr-AGT-1-2 which does not show significant age-related hypermethylation.  
119 We observe a similar pattern of sharp peaks of significance closely localised around the other loci in the  
120 study-wide significant set. GENCODE 19 places tRNA-Ile-AAT-4-1 in the 3'UTR of a Nonsense-mediated decay  
121 transcript of *CTC1* (CST Telomere Replication Complex Component 1, CTC1-002, ENST00000449476.2) and  
122 not of its primary transcript.  
123

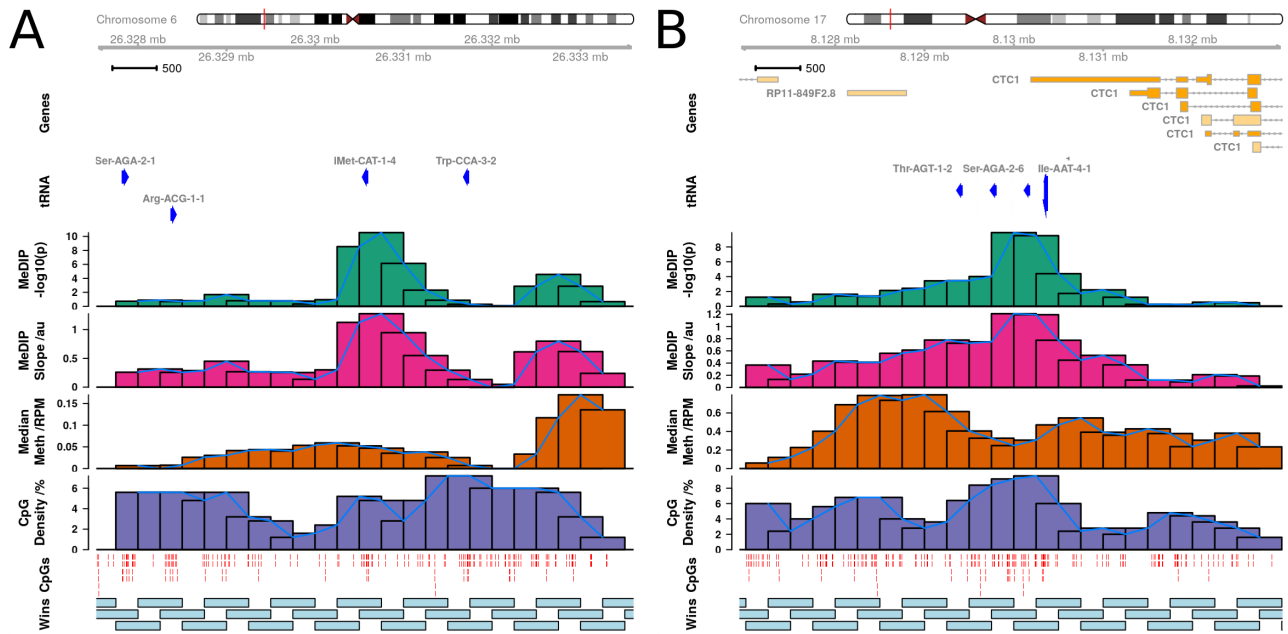


**Fig 3.** MeDIP-seq results (blood cell-type corrected model) for **A)** tRNA-iMet-CAT-1-4 as well as **B)** tRNA-Ser-AGA-2-6 and tRNA-Ile-AAT-4-1 exhibiting ageing-related DNA hypermethylation. Top to Bottom: Chromosome ideogram; Gene locations (GENCODE 19); MeDIP-seq DNA methylation ageing  $-\log_{10}(p)$  results (shown for each 500 bp overlapping window); MeDIP-seq slope of change with age; MeDIP-seq Medium coverage (Reads per Millions, RPM) calculated across all samples; CpG density (%); CpG locations (red lines); 500bp overlapping windows. The sharp peaks suggest that the results are localised to individual tRNA genes not the entire genic locus. One window overlapping tRNA-Ile-AAT-4-1 also partially overlaps tRNA-Ser-AGA-2-6. The 3' UTR of the CTC1 transcript CTC1-002 (ENST00000449476.2, GENCODE 19), which is subject to nonsense mediate decay, overlaps tRNA-Ile-AAT-4-1. tRNA genes with similar CpG density are exhibiting differing age-related DNAm change patterns.

To place these hypermethylating tRNA genes in their genomic context we examined how the extended set of 44 non-blood cell-type corrected study-wide significant tRNAs clustered with other tRNA genes. We clustered the tRNA genes by grouping together all tRNAs within 5Mb of one another and then required that a cluster contain at least 5 tRNA genes with a density of at least 5 tRNA genes per Mb (see Methods). This yielded 12 major tRNA gene clusters containing a total of 353 tRNA genes, 42 of the 44 study-wide significant tRNA genes within these clusters (Figure 4a). The hypermethylating tRNA genes are spread evenly among these clusters proportionately to their size (% ageing tRNA per cluster; non-significant one-way ANOVA).

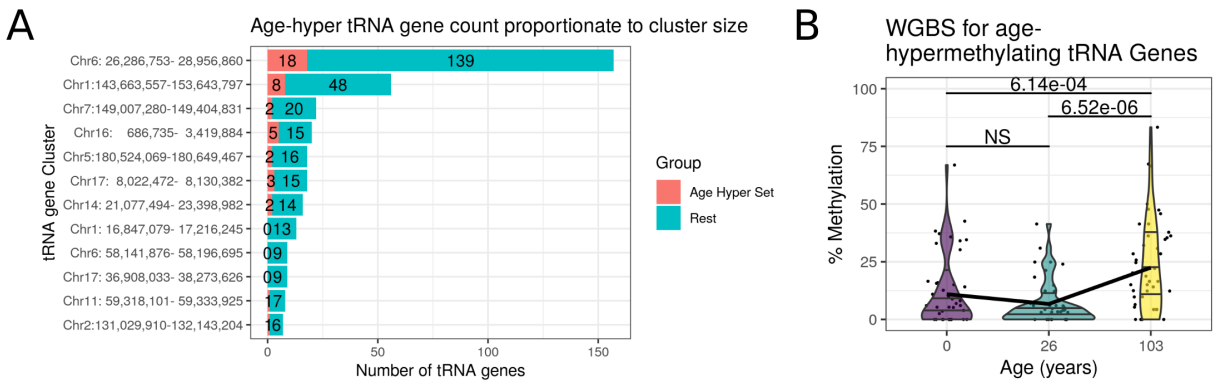


**Fig 4.** **A)** Covered study-wide significant tRNA genes ( $n = 14/16$ ) are more methylated in a centenarian than in a neonate or an adult (26 year) in Whole Genome Bisulfite Sequencing (WGBS) data from Heyn et al. [50]. Each point represents individual CpG methylation levels within a tRNA gene. **B)** No significant clusters of ageing-related tRNA. Proportion of non-blood cell corrected ageing-related study-wide significant tRNAs (42/44, red) within tRNA clusters (tRNAs within 5Mb with  $>5$  tRNA genes/Mb, see Methods).

## Age-related tRNA gene set DNA Hypermethylation is even observed in one Newborn versus one Centenarian

We examined an available Whole Genome Bisulphite sequencing (WGBS) dataset from Heyn *et al.* [50] (see Methods) These data consisted of blood-derived DNA WGBS in one newborn child and one 26 year old, and centenarian (103 years). In their analysis, the centenarian was found to have more hypomethylated CpGs than the neonate across all genomic compartments, including promoters, exonic, intronic, and intergenic regions. However, even in this examination of 3 individuals of 3 different age in the 55% of tRNA that possessed coverage, we observed DNA hypermethylation with age among the study-wide significant hypermethylating tRNA genes. The centenarian was significantly more methylated in this set of tRNAs than the neonate (Wilcoxon rank sum test, 6.14% increase (95% CI -Inf - 4.31),  $W = 717$ ,  $p = 6.14 \times 10^{-4}$ , see Figure 4b).

## Age-related Changes Independently Replicated with Targeted Bisulfite Sequencing

In order to further robustly support these-ageing related changes, we attempted to replicate these findings ourselves in an independent ageing dataset. Furthermore, we employed a different technology targeted bisulfite (BiS) sequencing to also further validate the MeDIP-seq-derived results. These data provide individual CpG resolution to identify what may be driving the regional DNAm changes observed, and precise quantitation of the magnitude of change.

We performed this targeted BiS-seq in blood-derived DNA from 8 pools of age-matched individuals at 4 time-points (~4, ~28, ~63, ~78 years) from a total of 190 individuals, as detailed in Table 1. This approach permitted us to assay tRNA gene DNA methylation across a large number of individuals whilst requiring a minimal amount of DNA from each (80-100ng), and costing ~1/24th as much as performing sequencing individually. A total of 79 tRNA loci generated reliable results post-QC (see Methods). These tRNAs covered a total of 458 CpGs with a median of 6 CpGs per tRNA (range 1-9). Median Coverage per site across pools, technical replicates and batches was 679 reads (mean 5902).

Firstly, we ran the 8 Pooled samples on the Illumina EPIC (850k) array to confirm that our pooling approach was applicable for DNAm ageing-related evaluation. This showed an  $R^2 = 0.98$  between pool mean chronological age and Horvath clock DNAm predicted age [11](see Figure 5c). Therefore, this confirmed the utility of our pooling approach. We also used these array derived data to estimate the major blood cell proportions for each of these pools with the Houseman algorithm [51].

**Table 1.** Summary information on participants in each pool. Total of 190 participants in 8 pools, at 4 time points: 4, 28, 63, & 78 years

Pool	Mean Age	Sex	Min Age	Max Age	n
Pool 1	4.07	Male	3.99	4.38	20
Pool 2	4.09	Female	3.99	4.36	20
Pool 3	28.07	Female	25.87	29.80	25
Pool 4	28.23	Female	26.05	30.01	25
Pool 5	63.40	Female	62.80	63.80	25
Pool 6	63.26	Female	62.70	63.70	25
Pool 7	77.96	Female	75.50	80.50	25
Pool 8	77.22	Female	74.40	80.10	25

**Table 2.** Pairwise Differences in Methylation between Age groups by tRNA. p-values are for pairwise methylation differences (see Methods)[52].

tRNA	num. CpGs	comparison	p-value	delta
tRNA-Ile-AAT-4-1	8	4 vs. 28	1.518e-01	-0.2
		4 vs. 63	1.774e-01	-0.234
		4 vs. 78	3.060e-01	0.0113
		28 vs. 63	7.152e-01	-0.0334
		28 vs. 78	1.553e-01	0.212
		63 vs. 78	2.057e-01	0.245
tRNA-iMet-CAT-1-4	5	4 vs. 28	8.403e-02	0.0116
		4 vs. 63	1.716e-01	0.0125
		4 vs. 78	1.997e-04*	0.0368
		28 vs. 63	3.943e-01	0.000869
		28 vs. 78	1.724e-02*	0.0252
		63 vs. 78	6.224e-02	0.0243
tRNA-Ser-AGA-2-6	9	4 vs. 28	4.222e-01	0.0573
		4 vs. 63	3.968e-01	0.0274
		4 vs. 78	4.651e-01	0.0423
		28 vs. 63	1.095e-01	-0.0299
		28 vs. 78	2.126e-01	-0.015
		63 vs. 78	2.201e-01	0.0149

We noted that individual tRNA loci exhibiting age-related changes in DNAm had duplicate or isodecoder (same anticodon but body sequence variation) sequences in the genome, which despite exact or near sequence identity did not show similar changes. tRNA-iMet-CAT-1-4 for instance is 1 of 8 identical copies in the genome and was the only locus that showed significant changes. The results of pairwise differential methylation tests between age groups for the 6 top tRNAs from the MeDIP-seq models are listed in Table 2. tRNA-iMet-CAT-1-4 shows a pairwise increase of 3.7% from age 4 years to age 78 years.

Of the 3 top hits in MeDIP-seq, tRNA-iMet-CAT-1-4 (Figure 5a(iii)) and tRNA-Ser-AGA-2-6 (Figure 5a(viii)) exceeded nominal significance ( $p\text{-values} = 9.35 \times 10^{-4}$  &  $4.28 \times 10^{-2}$ , respectively). However, tRNA-Ile-AAT-4-1 (Figure 5a(xi)) showed a nominal decrease in DNAm with age. tRNA tRNA-Leu-TAG-2-1

from the study-wide significant set also showed nominally significant hypermethylation with age (Figure 168  
5a(xviii)). Also, four of the individual CpGs in tRNA-iMet-CAT-1-4 exhibited nominally significant increases in 169  
DNAm with Age (Figure 5b). 170

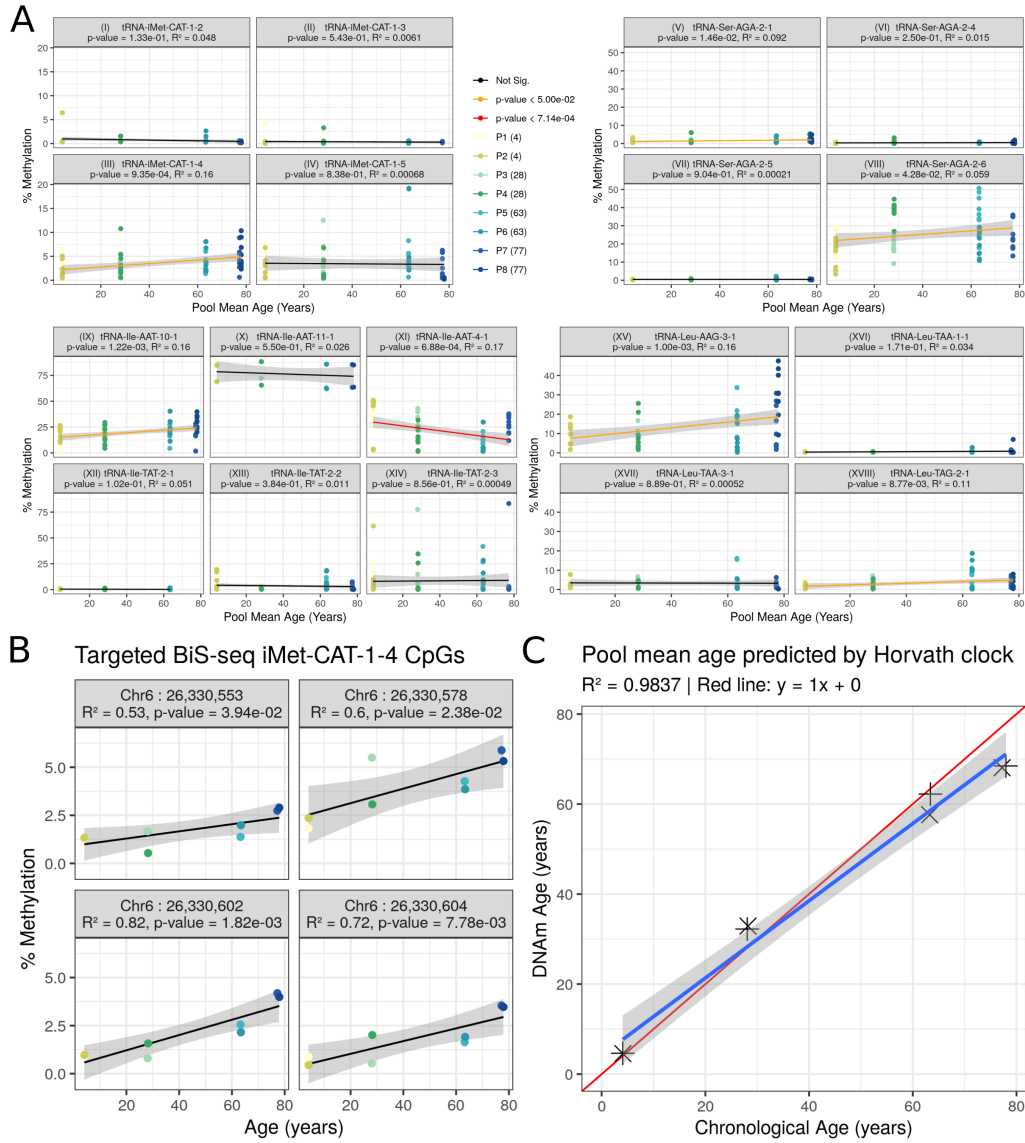


**Fig 5. Comparison of age-related hypermethylating tRNA genes to closely related tRNA genes using targeted bisulfite sequencing (BiS-seq).** **A**) Combined CpGs within tRNA loci results (experiment-wide Bonferroni  $p = 7.14 \times 10^{-4}$ ); *i-iv*, Comparison of select tRNA-iMet-CAT loci: Hypermethylation is specific to iMet-CAT-1-4 (iii) not other isodecoders (i, ii, & iv); *v-viii*, Comparison of select tRNA-Ser-AGA loci: Hypermethylation is specific to Ser-AGA-2-6 A (viii) and to a lesser extent Ser-AGA-2-1 (v), whilst not other isodecoders (vi, vii); *ix-xiv*, Comparison of select tRNA-Ile loci: Hypermethylation is specific to Ile-AAT-10-1 (ix), Ile-AAT-4-1 (xi) displays hypomethylation contrary to previous MeDIP findings, Ile-TAT-2-2 & 2-3 lack hypermethylation (previously non-significant in blood-corrected MeDIP, although significant in uncorrected), whilst no change in Ile-AAT-11-1 (x) and Ile-TAT-2-1 (xii); *xv-xviii*, Comparison of select tRNA-Leu loci: Hypermethylation in Leu-AAG-3-1 (xv) consistent with 450k and Leu-TAG-2-1 (xviii) consistent with MeDIP, whilst no change in Leu-TAA-1-1 (xvi) & Leu-TAA-3-1 (xvii). **B)** tRNA-iMet-CAT-1-4 Individual CpG analysis: 4 CpGs within this tRNA show consistent methylation increases (all  $p < 0.05$ ). **C)** Mean chronological age is tightly correlated with DNAm Horvath clock [11] predicted age for the 8 pooled samples (see Table 1 for pool details).

**Select Duplicates & Isodecoders of Hypermethylating tRNA loci remain unchanged** We targeted 171 a selection of these duplicate and isodecoder loci for bisulfite sequencing in order to confirm that the identified 172 DNA changes are specific to a given locus and not general to related tRNAs. Examining the tRNA-iMet-CAT-1 173 family, only the previously identified 1-4 version confirmed significant hypermethylation (not 1-2, 1-3 or 174 1-5)(Figure 5a(i-iv)). Likewise the tRNA-Ser-AGA-2-6 version was supported compared to 2-1,2-4 and 2-5(Figure 175 5a(v-viii))). Full Age model results are available in Supplementary File S2. 176

### DNA methylation 450k Array Data Validates the MeDIP-seq Results 177

Although DNA methylation array poorly covers the tRNA gene set, we wished to attempt to see if this BiS-based 178 but differing and well-established technology was supportive at all of our DNA hypermethylation findings. 179 TwinsUK had available 450k array on 587 individuals, and this platform includes 143 probes, covering 103 180 tRNAs. All the 3 top tRNAs in the MeDIP-seq results were covered by this data set, and 7 of the 16 study-wide 181 significant set. 9 tRNAs show significant ( $p < 4.58 \times 10^{-4}$ ) increases in DNA methylation with age in models 182 corrected for blood cell counts including all 3 of the 3 tRNAs identified in the MeDIP-seq as genome-wide 183 significant and 5 of the 7 study-wide significant set present on the array (Figure 6). Although it should be noted 184 that 56 of these 143 probes are within the non-robust set of Zhou et al. [42], including 1 of the genome-wide, and 185 1 of the study-wide results (covering tRNA-Ile-AAT-4-1 & tRNA-Val-AAC-4-1), respectively. Full age model 186 results for all tRNA probes are provided in Supplementary File S3. 187

## Age-related DNA methylation change in tRNA genes

Twins UK - Illumina 450k array

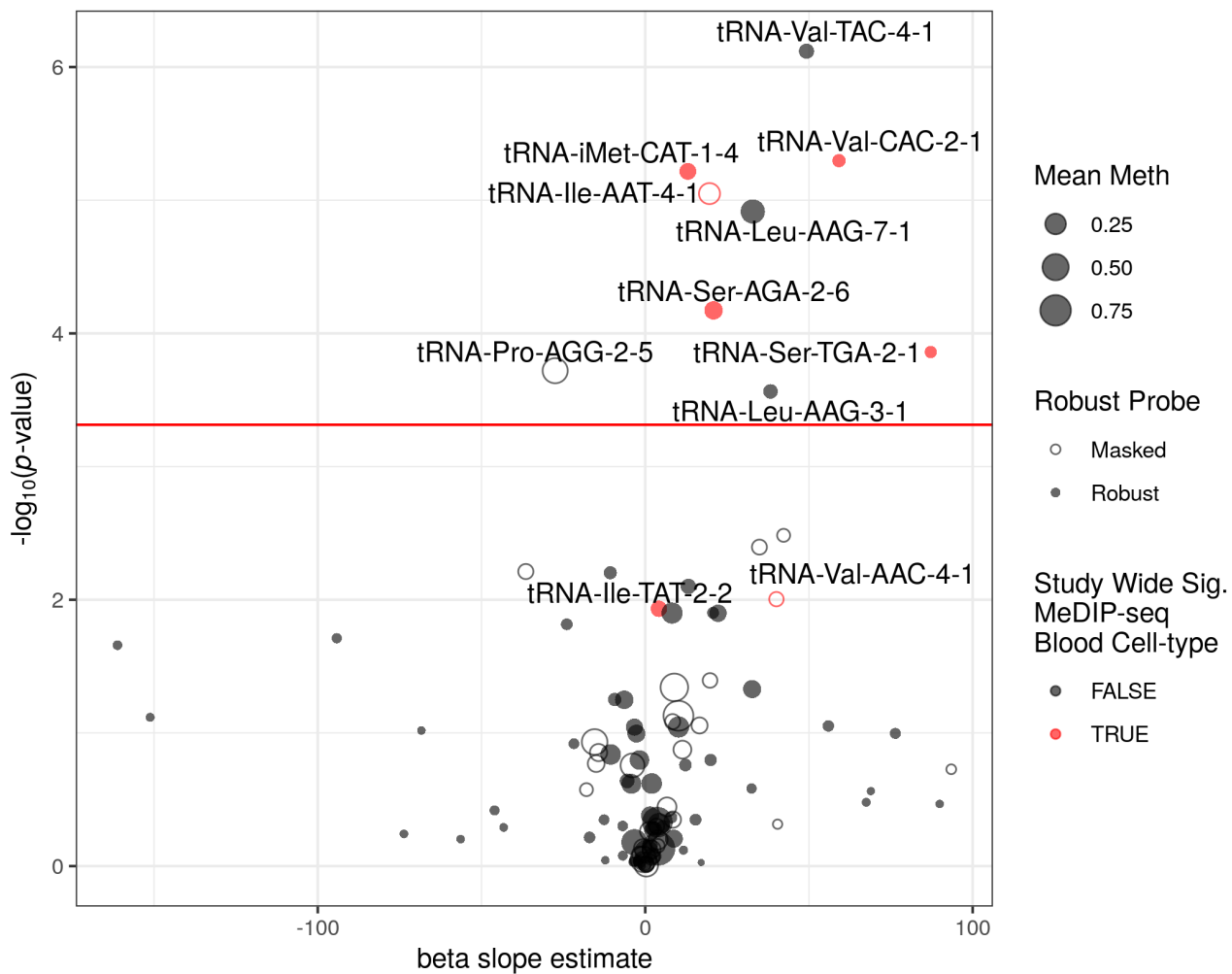


**Fig 6. Age-related DNA methylation change in tRNA genes** Five of seven tRNAs study-wide significant in MeDIP covered by the 450k array also show significant hypermethylation in this data. tRNAs are labelled if they are significant here or were in the MeDIP-seq data (Red). Model slope: the model coefficient for the methylation values. Unfilled circles indicate those probes with potential issues generated by Zhou et al. [42], this includes tRNA-Ile-AAT-4-1. Significance threshold:  $0.05/103 \approx 4.58 \times 10^{-4}$  (the number of tRNA genes examined).

### Ageing-Related tRNA Loci show increased Enhancer-Related Chromatin Signatures

We further explored the activity of the tRNA genes in public Chromatin segmentation data in blood (Epilogs 189 Blood & T-cells set) [53,54]. This shows proportionally more Enhancer-related (Enh, EnhBiv & EnhG) 190 chromatin states at tRNA genes hypermethylating with age than the stronger Promoter-related (TSS) in other 191 tRNAs. (Figure 7 b). Whereas these characteristics are less frequently predominant in the rest of the tRNAs 192 (Figure 7 b). Age-hypermethylating tRNA are enriched for enhancer chromatin states compared to the rest of the 193

tRNA genes (Fisher's Exact test  $p = 0.01$ ).

194

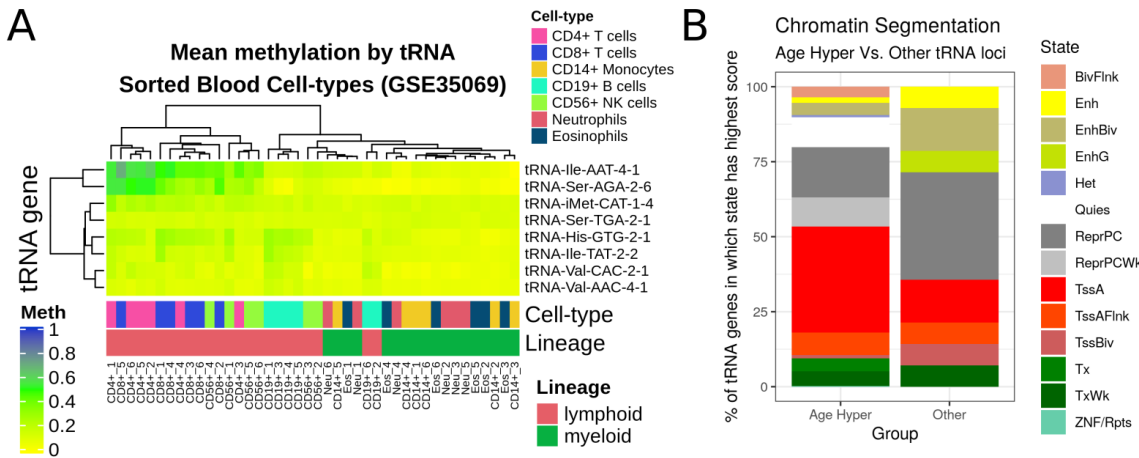


**Fig 7. A)** Heatmap of Mean DNA methylation of tRNA sorted Blood Cell Types (data from Reinus et al., probes covering 8 of the 16 study-wide significant tRNA in 7 cell-type fractions from 6 males via GSE35069, [55,56]). This illustrates the ability of tRNA gene methylation to separate the myeloid from the lymphoid lineage and the higher methylation in the lymphoid lineage of the 3 cell-type corrected genome-wide significant tRNAs (iMet-CAT-1-4, etc.) **B)** Chromatin Segmentation data for 'Blood & T-cell' from Epilogos 15 State model [53,54]. Proportion represents the frequency of the predominant chromatin state at a given tRNA (+/- 200bp) for 14/16 study-wide significant tRNAs covered compared to other 371 available tRNAs. The ageing-related hypermethylated tRNAs are enriched for enhancer chromatin state (Fisher's Exact  $p = 0.01$ ).

### Age Hypermethylating tRNAs are more methylated in Lymphoid than Myeloid cells

195

Three tRNA genes remained genome-wide significant and 16 study-wide significant following correction for major cell-type fraction. This is suggestive of either cell-type independent change or, presumably less likely, a very large effect in a minor cell-type fraction. tRNAs have exhibited tissue-specific expression [57–59] and blood cell-type populations change with age. Specifically, there is shift to favour the production of cells in the myeloid lineage [47]. These points lead us to examine tRNA gene DNAm in sorted cell populations. We used a publically available 450k array dataset [55]) that has been used in the construction of cell-type specific DNAm references for cell-type fraction prediction using the Houseman algorithm [51] (see Methods). This consists of data from 6 individuals (aged  $38 \pm 13.6/\text{yrs}$ ) from seven isolated cell populations (CD4+ T cells, CD8+ T cells, CD56+ NK cells, CD19+ B cells, CD14+ monocytes, neutrophils, and eosinophils). We found that tRNA gene DNAm could separate myeloid from lymphoid lineages (Figures 7 a & S4).

196

197

198

199

200

201

202

203

204

205

Of the eight study-wide significant tRNAs with array coverage, we identified that collectively these eight are significantly more methylated in the lymphoid than the myeloid lineage (1.1% difference, Wilcoxon rank sum test  $p = 1.50 \times 10^{-6}$  95% CI 0.7%–∞). Thus, any age related increases in myeloid cell proportion would be expected to dampen rather than exaggerate the age-related hypermethylation signal that we observed. In addition

206

207

208

209

tRNA-Ile-AAT-4-1 and tRNA-Ser-AGA-2-6 have the highest variance in their DNAm of all 129 tRNAs covered in  
210 this dataset. This could represent ageing-related changes as these samples range across almost 3 decades.  
211

Another possibly may be that these loci as well as hypermethylating are also increasing their variability with age  
212 in a similar fashion to those identified by Slieker *et al.* [60]. In that study they identified that those loci accruing  
213 methylomic variability were associated with fundamental ageing mechanisms.  
214

## tRNA Genes also Hypermethylate with Age in Solid Tissue

215

Some tRNA gene expression has been shown to be highly tissue specific [57–59]. It follows that our observations  
216 of changes in DNAm with age in blood might be specific to that tissue. We used a mix of 450k and 27k array  
217 data from ‘solid tissue normal’ samples made available by TCGA (The Cancer Genome Atlas) and data from  
218 foetal tissue [61,62] downloaded from GEO (see Methods). The samples from TCGA range in age from 15–90 (n  
219 = 733). Only 43 tRNA genes had adequate data to compare across tissues in this dataset and 115 in the foetal  
220 tissue data.  
221

Only 2 of the 3 tRNA genes we identified as genome-wide significant and a further 1 of the study-wide  
222 significant tRNA genes are present in the set of 45 tRNA genes in the TCGA data, thus limiting our ability to  
223 draw conclusions about the tissue specificity of our results. Solid tissue samples have a strong preponderance for  
224 low levels of methylation consistent with the active transcription of many tRNA genes and show slight increasing  
225 methylation with age but age accounts for very little of the variance (linear regression slope estimate = 1.52;  
226  $R^2 = 0.0002$ ; p-value  $1.34 \times 10^{-3}$  (Figure S5d)). In a pan-tissue analysis we found that 10 tRNA genes showed  
227 changes in DNAm with age, 9 of which were hypermethylation (p-value  $< 1.1 \times 10^{-3}$ ). One of these tRNA genes,  
228 tRNA-Ser-TGA-2-1 was also present in study-wide significant set of tRNA genes. Figures S6 & S7 illustrate  
229 minimal tissue specific differences. Interestingly, however, tRNA-iMet-CAT-1-4 and tRNA-Ser-AGA-2-6  
230 appeared more variable in methylation state than many other tRNAs in the TCGA normal tissue samples  
231 (Figure S6) and indeed have the highest variance in DNA methylation across tissues (Figure S5c).  
232

## Mice also show age-related tRNA gene DNA hypermethylation

233

We examined the DNA methylation of the mouse tRNA genes in using data from a reduced representation  
234 bisulfite sequencing (RRBS) experiment performed by Petkovich et al. [63]. These data from 152 mice covered 51  
235 tRNA genes and 385 CpGs after QC (see Methods), representing ~11% of mouse tRNA genes. The mice ranged  
236 in age from 0.67–35 months.  
237

Three of the 51 tRNAs showed Bonferroni significant DNA methylation changes with age (p-value <  
238

$1.08 \times 10^{-4}$ ) and all were in the hypermethylation direction. These three are tRNA-Asp-GTC-1-12, 239  
tRNA-Ile-AAT-1-4, tRNA-Glu-TTC-1-3 (Figure 8). Full Age model Results are available in Supplementary File 240  
S4. 241

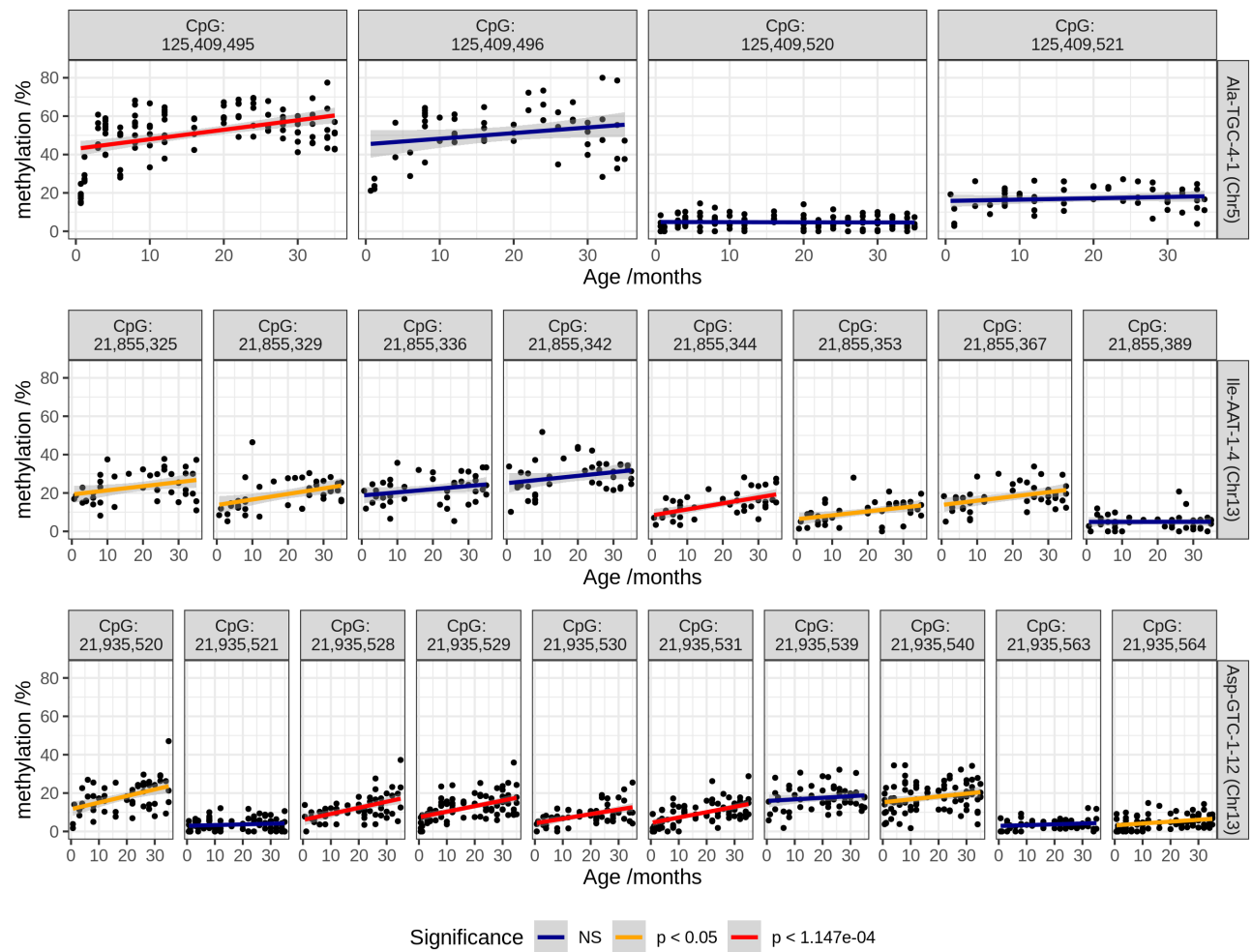


**Fig 8.** DNA methylation of CpGs in 3 tRNA which significantly hypermethylate with age in mice, in data from Petkovich et al. [63]. 6 CpGs reach bonferroni significance and 7 show nominally significant increases.

In order to investigate the mouse results further we made use of data from Thornlow et al. [64], which had 242 established tRNA ortholog sets for 29 mammalian species. They identified 197 mouse tRNAs as having direct 243 human orthologs with 44 of these included in the mouse results from Petkovich et al. [63]. However, 244 unfortunately, although 2 of the top 3 tRNAs (tRNA-Ser-AGA-2-6 & tRNA-Ile-AAT-4-1) have mouse orthologs 245 (tRNA-Ser-AGA-2-2 & tRNA-Ile-AAT-1-1), they are not covered in these mouse data. Furthermore, none of the 246 tRNAs showing significant hypermethylation in mice (at nominal  $p < 0.05$ ) had human orthologs in our 247 MeDIP-seq study-wide significant hypermethylating set. Therefore, whilst we cannot directly compare specific 248

tRNA loci due to this lack of coverage, it is interesting that the small number of significant tRNA genes in the  
249 mouse data also hypermethylate with age.  
250

## Discussion

251

Our work has identified a previously unknown enrichment for age-related epigenetic changes within the tRNA genes of the human genome. This observation was strongly directional with increasing DNA methylation with age [65]. The MeDIP-seq dataset employed brought advantages in exploring this undefined terrain of the human tRNA genes. Firstly, being genome-wide it provides much increased access, as these regions are poorly covered by current arrays. Secondly, being a fragment-based regional assessment of DNA methylation, the individual but highly similar small tRNA genes can be surrounded by unique sequence.

252  
253  
254  
255  
256  
257

We determined by genome-wide permutation that this strong hypermethylation signal was specific to the tRNA genes, and not merely driven by the underlying CpG density of these loci. A targeted BiS-seq experiment validated the defined nature of the tRNA change in an independent dataset, with a successful pooling approach, which may also be useful for other ageing-related targeted DNA methylome evaluations. Additionally, we gained support for our results from limited DNA methylation array data.

258  
259  
260  
261  
262

Whilst the changes in DNA methylation we have observed are relatively small (i.e. 3.7% between 4-year to 78-year pools in tRNA-iMet-CAT-1-4), this is consistent with the effect size seen in the majority of positions differentially methylated with age in many other studies [60,66], except for the noted extreme outliers, such as *EVOLV2* [67]. Furthermore, effect size cut-offs are observed to remove a large fraction of true age-DMPs [68].

263  
264  
265  
266  
267

We subsequently explored further what was driving this age-related phenomenon and its possible biological implications. As this result was observed in peripheral blood, we were well aware that we were examining DNA derived from a heterogeneous cell type population [69]. Moreover, that there are well known age-related proportional changes in peripheral blood cell composition [47]. The TwinsUK MeDIP-seq and 450k array DNA methylation data included measured haematological values. Therefore, we adjusted for major cell type effects, such as a myeloid skew, and distinct tRNAs were still significant. Although, a caveat to our study is that this can not exclude changes in minor specific sub-cell fractions types. However, that these age-related effects were strong enough to be observed in both a regional MeDIP-seq assessment and a pooled sequencing approach, implies that they not extremely subtle. We examined age-related tRNA gene DNA methylation changes in the limited subset of mouse tRNA genes covered in publicly available RRBS data (~13%) and were able to identify tRNAs exhibiting DNA hypermethylation with age in this set. This suggests that age-related tRNA gene hypermethylation may not be unique to humans, but at least observed across mammals.

268  
269  
270  
271  
272  
273  
274  
275  
276  
277  
278

Due to the high number of hypermethylating tRNAs prior to cell-type correction, we were also curious whether the epigenetic state of this small tRNA gene fraction of genome could capture and in fact be a defined fingerprint of cell type. We found that tRNA gene DNA methylation could separate myeloid from lymphoid lineages. There

279  
280  
281

was also some suggestion of more fine-grained blood cell-type signatures in tRNA DNAm, such as the separation  
282 of CD19+ B cells from CD4/8+ T cells. Ageing is also known to lead to an increase in senescent cells (*e.g.* CD8+  
283 CD28- cells). Whether these epigenetic changes in the tRNA genes uniquely represent these cell-types will  
284 require technical advances to enable future single cell DNA methylome analysis to accurately assess these regions.  
285 If further supported, the epigenetic state of these tRNA loci may aid the taxonomy of cell-type definition.  
286

We observed a predominantly unmethylated state across fetal (Figure S7) and adult tissues (Figure S6) at  
287 tRNA gene loci, consistent with the high rate of transcription at many tRNA genes. We suspect that the tRNA  
288 genes largely remain unmethylated through development and that the moderate increases in DNAm that we are  
289 observing with age at these loci are being driven by changes arising primarily in older individuals. Distinct  
290 biological changes have been observed recently in aged individuals [70,71]. Our data are supportive of the tRNA  
291 gene set representing a distinct functional unit, which lacks the logarithm change in the young observed strongly  
292 in CpGs employed in ‘clocks’ [13]. This would also be consistent with the lack of significant differences in the  
293 tRNA loci detected between the neonate and the 26-year-old adult in the Heyn et al. data. This low baseline  
294 DNA methylation of the tRNA genes may also explain why we predominantly observe hypermethylation with age.  
295 Whether this is driven by mechanisms, such as aberrant DNA methylation targeting of the tRNA loci or specific  
296 sub-celltype effects with age, will require further experimental investigation.  
297

This signal within the tRNA families was observed to occur at specific Isodecoders. Isodecoders expand in  
298 number with organismal complexity and the high prevalence in mammals has been suggested due to their  
299 additional regulatory functionality [72,73]. They also have distinct translational efficiency [74], which can also  
300 have consequences in human disease [75]. After correcting for major cell types, we identified 2 tRNA genes  
301 tRNA-iMet-CAT-1-4 and tRNA-Ser-AGA-2-6 which had the most consistent hypermethylation across 3 different  
302 assays. Regarding the inconsistent tRNA-Ile-AAT-4-1 result, it is covered by a MeDIP-seq 500bp window which  
303 exhibited genome-wide significant hypermethylation, but also partially overlaps tRNA-Ser-AGA-2-6 (Figure 3B).  
304 Whilst the 450k array probe overlapping tRNA-Ile-AAT-4-1 (cg06382303) appears to replicate this  
305 hypermethylation, it is a borderline case for exclusion flagged by Zhou et al. [42] due to non-unique 30bp 3'  
306 subsequence. In the targeted Bisulfite sequencing data, tRNA-Ile-AAT-4-1 exhibited a loss of methylation.  
307 Therefore, this may suggest that the hypermethylation signal observed at this locus in the MeDIP-seq data could  
308 have been ‘pulled up’ by the neighbouring tRNA-Ser-AGA-2-6 hypermethylation signal. Of the 16 study-wide  
309 significant tRNA genes, only these two of these have a shared significant window, furthermore, in the expanded  
310 set of 44 only tRNA-Thr-AGT-1-2 could be similarly affected.  
311

Furthermore, there is great complexity to the fragmentation of tRNA [23], with physiological processes such  
312 as stress shown to induce fragment production [76]. These resultant tsRNAs can feedback on protein synthesis by  
313

regulating ribosome biogenesis [77] and others have diverse regulatory functions such as targeting transposable element transcripts [78]. They are also observed to circulate in the blood in a cell-free fashion, and fragment levels can be modulated by ageing and calorie restriction [41]. The isodecoder specific nature of our findings frame a possible hypothesis for regulatory change with age and future work will be required to unravel this potential. tsRNA abundance has been associated with locus specific tRNA gene expression, in some cases independent of mature tRNA levels [79]. This has important implications for the interpretation of our results given the multi-copy nature of genes like tRNA-iMet-CAT-1-4, as even if expression levels of mature iMet tRNAs are unaffected by changes in one copy's DNA methylation, these changes could still influence the levels of particular tsRNAs derived from specific tRNA loci.

The location of tRNA-Ser-AGA-2-6 and tRNA-Ile-AAT-4-1 immediately downstream of *CTC1* and of tRNA-Ile-AAT-4-1 within the 3'UTR of an alternate isoform of *CTC1*, which undergoes nonsense-mediated decay, raises the possibility that the gene body epigenetic regulation of *CTC1* may impact on the state of these tRNA genes. *CTC1*'s function in telomere maintenance [80], DNA replication licensing [81], and it's role in a rare progeroid condition [82] indicate that it has ageing-relevant biology. The possible relationship between the regulation of *CTC1* and that of the tRNA genes downstream of it warrants further study.

Whilst, the expression of the tRNA genes has long been simplified as 'constitutive', some observations have indicated that many tRNA genes are expressed in a tissue-specific fashion in diverse organisms [58,59]. Although others have found the majority of isodecoders are transcribed in different cell types [28]. Several transcription factors acting via TFIIIB [83] have a negative (the tumour suppressors p53 [84] and Rb [85]) or positive (the proto-oncogene c-Myc) influence [83]. Regulatory sequence in the flanking or the internal regions of tRNA genes do not explain tRNA expression variation [86]. Whilst DNAm is able to repress the expression of tRNA genes [32], the broader chromatin environment also affects tRNA transcription. Due to the co-ordinated nature of epigenomic modifications, it may also be revealing to evaluate ageing-related histone modification in these tRNA loci. Furthermore, recent data from Gerber et al [87] indicates Pol-II may also have a dynamic regulatory role in tRNA expression.

Changes in the epigenetic state of specific tRNA could be modulating transcription efficiency or even codon availability in the ageing cell. tRNA gene dosage is quite closely matched to amino acid usage frequency in the human exome. However, the transcriptome codon usage frequency and tRNA gene expression have been claimed to vary with the replicative state of cells, separating differentiated from replicating cells [88]. Others have argued that these differences are substantially explained by variation in GC content [89] and that codon usage frequencies are observed to be mostly invariant in the transcriptomes of a wide range of tissues, as well as across developmental time [86]. Although, experimental stress-related states have revealed changes with an

over-representation of codons that are translated by rare tRNAs [90].

tRNA sequences themselves are under strong structural (both secondary and tertiary) [72] as well as functional constraint, which leads to an order of magnitude reduction in variation compared the background genomic mutation rate [28]. Despite strong purifying selection maintaining very low variation in tRNA gene bodies, tRNA genes are subject to high levels of transcription-associated mutagenesis (TAM) leading to elevated mutation rates over evolutionary time in their immediate flanking sequences [91]. The possible effects of genetic variation on DNA methylation mean that polymorphic tRNA could be another potential caveat to our work. Although, there is no significant population variation in, for example, tRNA iMet sequences in 1,000 Genomes data. Indeed, there are only 11 new isodecoder sequences with high confidence (tRNAscan scores  $\geq 50$ ) at  $>1\%$  population frequency [28]. There is also some evidence for tRNA copy number variation at specific loci, although this remains under-characterised [92,93]. Another potential cause we considered was whether age-related somatic copy number increases could be occurring in these loci. Population or somatic copy number expansions could lead to increased methylated reads in MeDIP-seq without any epigenetic state change. However, this would not be consistent with the targeted and array BiS conversion methodologies, where the proportion of methylated to unmethylated reads would still be constant.

It is worth noting the parallels with known cancer and ageing epigenetic changes, and that tRNAs are also dysregulated in cancer [94], with proposed utility as prognostic markers [95]. Furthermore, the early replicating state of tRNA loci, potentially associated with high expression [96], may make them prone to hypermethylate, as is observed in early replicating loci in both cancer [97] and senescent cells [98]. Interestingly, tRNA gene loci may also play a role in local as well as large scale genome organisation [43]. tRNA gene clusters act as insulators [99] and have extensive long-range chromatin interactions with other tRNA gene loci [43]. The coordinated transcription of tRNAs at subnuclear foci and the B-box sequence elements bound by TFIIIC and not PolIII may represent an organising principle for 3D-chromatin by providing spatial constraints [100]. Therefore, these tRNA epigenetic changes could contribute to the structural changes that are also observed in ageing [101].

In conclusion, due to the unique challenges that make the tRNA genes difficult to examine it has remained epigenetically under-characterised despite its critical importance for cell function. We directly interrogated the epigenetic DNA methylation state of the functionally important tRNA genes, across the age spectrum in a range of datasets as well as methodologies and identified an enrichment for age-related DNA hypermethylation in the human tRNA genes.

## Methods

375

### Participants

376

Participants in the ‘EpiTwins’ study are adult volunteers from the TwinsUK Register. The participants were aged between 16 and 82 years, with a median of ~55 years (cohort profile [102]). Ethics for the collection of these data were approved by Guy’s & St Thomas’ NHS Foundation Trust Ethics Committee (EC04/015—15-Mar-04) and written informed consent was obtained from all participants.

377

378

379

380

Participants for our targeted bisulfite sequencing of select tRNA loci were drawn from two studies. Samples from participants aged 4 and 28 years are from the MAVIDOS [103] study and participants aged 63 and 78 years are from the Hertfordshire cohort study [104]. Due to a limited number of available samples, the two 4 year old pools contained DNA from 20 individuals each, with all other pools having 25 contributing individuals. Pool 1, the first 4 year old pool used DNA from all male samples, with all other pools using all female samples. Thus, the total number of participants was 190 (see Table 1). Samples from the 28 year old time point are all from pregnant women at ~11 weeks gestation.

381

382

383

384

385

386

387

### tRNA annotation information

388

Genomic coordinates of the tRNA genes were downloaded from GtRNAdb [27]. The 2 tRNAs located in chr1\_gl000192\_random are tRNA-Gly-CCC-8-1 & tRNA-Asn-ATT-1-2 (Supplementary File S5). The 213 probes overlapping tRNA genes were derived from intersecting the tRNA gene annotation data from gtRNAdb with the Illumina 450k array manifest annotation for the hg19 genome build using `bedtools` v2.17.0 [105]. We excluded 107 tRNAs from blacklisted regions of hg19 [46].

389

390

391

392

393

### tRNA Gene Clustering

394

We clustered the tRNA genes by grouping together all tRNAs within 5Mb of one another using the `bedtools merge` tool v2.17.0 [105]. We used a command of the form: `bedtools merge -c 4 -o collapse -d <N> -i hg19-tRNAs.bed` where <N> is the binsize. We varied the binsize and selected 5Mb as it is at approximately this size that number of clusters with more than one tRNAs exceeds the number of singleton tRNAs (Figure S9). We added the further requirements that these groupings contain at least 5 tRNA genes with a density of at least 5 tRNA genes per Mb to be considered as clusters.

395

396

397

398

399

400

## DNA methylome data

401

### TwinsUK MeDIP-seq methylomes

402

The Methylated DNA Immunoprecipitation sequencing (MeDIP-seq) data was processed as previously described [16,106]. These processed data are available from the European Genome-phenome Archive (EGA) (<https://www.ebi.ac.uk/ega>) under study number EGAS00001001910 and dataset EGAD00010000983. The dataset used in this work consists of 4350 whole blood methylomes with age data. 4054 are female and 270 male. 3001 have full blood counts. There are 3652 individuals in this data set. These individuals originate from 1933 unique families. There are 1234 monozygotic (MZ) twin pairs (2468 individuals), and 458 dizygotic (DZ) twin pairs (916 individuals).

403

404

405

406

407

408

409

MeDIP-seq used a monoclonal anti-5mC antibody to bind denatured fragmented genomic DNA at methylated CpG sites. This antibody-bound fraction of DNA was isolated and sequenced [44]. MeDIP-seq 50-bp single-end sequencing reads were aligned to the hg19/GRCh37 assembly of the human genome and duplicates were removed. MEDIPS (v1.0) was used for the MeDIP-seq specific analysis [107]. This produced reads per million base pairs (RPM) values binned into 500bp windows with a 250bp slide in the BED format, resulting in ~12.8 million windows on the genome. MeDIP-seq data from regions of interest was extracted using Bedtools v2.17.0 [105].

410

411

412

413

414

415

### Analysis of DNA methylome data for Significant Ageing-related changes

416

All analysis was performed in R/3.5.2. Linear models were fitted to age using the MeDIP-seq DNA methylome data, as quantile normalised RPM scores at each 500bp window. Models were fitted with: 1. No covariates; 2. Batch information as a fixed effect; 3. Blood cell-type counts for neutrophils, monocytes, eosinophils, and lymphocytes as fixed effects; and 4. Batch and Blood Cell counts as fixed effects. Model 1 & 2 were fitted on the full set of 4350 as batch information was available for all samples but blood cell count data was only available for a subset of 3001 methylomes. Models 1 & 2 fitted in the n=3001 subset were similar to those fitted in the complete set of 4350. Models 3 & 4 were fitted in the n=3001 subset with full covariate information and sets of significant tRNAs identified at study-wide and genome wide levels in model 4 were used in subsequent analyses. Models were also fitted for two unrelated subsets created by selecting one twin from each pair (Monozygotic or Dizygotic), yielding sets with n = 1198 & 1206 DNA methylomes. One additional model was fitted for longitudinal analysis, samples were selected by identifying individuals with a DNA methylome at more than one time point and filtering for only those with a minimum of 5 years between samples. This yielded 658 methylomes from 329 individuals with age differences of 5-16.1 yrs, median 7.6 yrs. Models for this set included participant identifier as a fixed effect in addition to blood cell counts and batch information.

417

418

419

420

421

422

423

424

425

426

427

428

429

430

## Permutation Analysis for Enrichment with Age-related Changes

431

We performed a permutation analysis to determine whether the CpG distribution of sets of the tRNA genes was 432  
the principle driver of the ageing-related changes observed. Windows overlapping tRNAs have a higher 433  
proportion of windows with a greater CpG density than their surrounding sequences (see supplementary Figure 434  
S8). CpGs residing within moderate CpG density loci are the most dynamic in the genome [48] and CpG dense 435  
CpG island regions include specific ageing-related changes [8,9,16]. For comparison we also performed the 436  
permuation in the CGI regions from the Polycomb group protein target promoters in Teschendorff *et al.* [8] and 437  
bivalent loci from ENCODE ChromHm ‘Poised Promoter’ classification in the GM12878 cell-line [54]. A 438  
random set of 500bp windows representing an equivalent CpG density distribution of the feature set in question 439  
were selected from the genome-wide data. Above a certain CpG density there are insufficient windows to sample 440  
without replacement within a permutation. Furthermore, above  $\sim \geq 18\%$  CpG density CpG Islands become 441  
consistently hypomethylated [108]. Therefore, all windows with a CpG density of  $\geq 18\%$  (45 CpGs per 500bp) 442  
were grouped and sampled from the same pool. i.e. a window overlapping a tRNA gene which had a 20% density 443  
could be represented in permutation by one with any density  $\geq 18\%$ . This permutation was performed 1,000 444  
times to determine an Empirical p value by calculating the number of times the permutation result exceeded the 445  
observed number of significant windows in the feature set. *Empirical p – value* =  $\frac{r+1}{N+1}$ , where r is the sum of 446  
significant windows in all permutations and N is number of permutations [109]. 447

## Neonate and Centenarian Whole Genome Bisulfite Sequencing

448

DNA methylation calls were downloaded from GEO:GSE31263 and intersected with tRNA genes using bedtools 449  
v2.17.0 [105]. 450

## Sample pooling and EPIC array

451

We performed an Illumina Infinium DNA methylation EPIC array ((C) Illumina) and targeted bisulfite 452  
sequencing of select tRNA gene loci. Here we used DNA extracted from whole blood and pooled into 8 samples 453  
from unrelated individuals at 4 time-points with 2 pools at each time-point. The timepoints were 4, 28, 63, and 454  
78 years. Using the EPIC array we were able to infer the DNAm age using the Horvath DNAm clock [11] and 455  
blood cell-type composition of our samples using the Houseman algorithm [51]. 456

## Targeted Bisulfite Sequencing

457

We selected tRNA loci for targeted sequencing in which have had observed changes and DNA with age and closely related tRNAs in which changes were not observed. Primer design was performed using ‘methPrimer’ [110] (Supplementary File S6). A total of 84 tRNA loci were targeted and 79 subsequently generated reliable results post-QC. The targeted tRNAs covered a total of 723 CpGs with a median of 8 CpGs per tRNA (range 1-13), data passing QC was generated for 458 CpGs, median 6 (range 1-9) per tRNA.

458

459

460

461

462

Quality was assessed before and after read trimming using `fastqc` [111] and `multiqc` [112] to visualise the results. Targeting primers were trimmed with `cutadapt` [113] and a custom `per15` script. Quality trimming was performed with `trim_galore` [114]. Alignment and methylation calling was performed with `Bismark` (v0.20.0) [115] making use of `bowtie2` [116]. The alignment was performed against both the whole hg19 genome and just the tRNA genes +/- 100bp to assess the possible impact of off-target mapping. Mapping to the whole genome did produce purported methylation calls at a larger number of loci than mapping just to the tRNA genes (683,783 vs 45,861 respectively). Introducing a minimum coverage threshold of 25 reads dramatically reduced this and brought the number of sites into line with that in the tRNA gene set (36,065 vs 33,664 respectively) suggesting a small number of ambiguously mapping reads. All subsequent analysis was performed using the alignment to just the tRNA genes with a minimum coverage of 25 reads.

463

464

465

466

467

468

469

470

471

472

We performed pairwise differential methylation analysis of the tRNA genes at the different time points using `RnBeads` [52] with `limma` [117] and a minimum coverage of 25 reads. We also performed linear regression predicting age from DNA methylation at the targeted tRNA sites, permitting us to compare rates of increase with age. For the linear regression, we used only CpG sites with more than 25 reads mapped to the regions of the genome targeted for amplification.

473

474

475

476

477

## TwinsUK Illumina 450k array methylomes

478

Illumina Infinium DNA methylation 450k arrays ((C) Illumina) were also performed on TwinsUK participants, in 770 Blood-derived DNA samples which had matched MeDIP-seq data. These data were preprocessed in the form of methylation ‘beta’ values pre-processed as previously described [16,106]. Cell-type correction was performed using cell-count data and the following model: `lm(age ~ beta + eosinophils + lymphocytes + monocytes + neutrophils)`.

479

480

481

482

483

<b>Chromatin Segmentation Data</b>	484
Epilogs chromatin segmentation data [53] was downloaded for the tRNA gene regions +/- 200bp from <a href="https://explore.altius.org/tabix/epilogos/hg19.15.Blood_T-cell.KL.gz">https://explore.altius.org/tabix/epilogos/hg19.15.Blood_T-cell.KL.gz</a> using the <b>tabix</b> utility. The data used was the ‘Blood & T-cell’ 15 State model based on segmentation of 14 cell-types. This data was manipulated and visualised with R and <b>ggplot2</b> .	485 486 487 488
<b>Isolated Blood Cell Type Specific Data</b>	489
Data from 7 cell-type fractions from 6 Male individuals was downloaded from GSE35069 [55] using <b>GEOquery</b> [118]. Five of the 6 top age hypermethylating tRNAs are covered by this array dataset. Heatmaps were created with the <b>ComplexHeatmap</b> R package [56].	490 491 492
<b>Cancer and Tissue Specific Methylation Data</b>	493
Data was downloaded from the TCGA (The Cancer Genome Atlas) via the GDC (genomic data commons) data portal [119] using the <b>GenomicDataCommons</b> R package. Data from foetal tissue [61,62] was downloaded from GEO (GSE72867, GSE30654). From the TCGA, we selected samples for which DNAm data was available from both the primary site and normal solid tissue, and for which we could infer an approximate age (within one year). We selected those probes overlapping tRNA genes yielding 73,403 data points across 19 tissues with an age range of 15-90yrs (median 63.4) (Supplementary File S7)	494 495 496 497 498 499
<b>Mouse RRBS Analysis</b>	500
We downloaded methylation calls and coverage information resulting from RRBS performed by Petkovich <i>et al.</i> [63] from GEO using <b>GEOquery</b> [118] GSE80672. These data from 152 mice covered 68 tRNA and 436 CpGs after QC requiring >50 reads per CpG and >10 data points per tRNA. We excluded 5 tRNAs from blacklisted regions of mm10 [46]. After QC there were 58 tRNA genes and 385 CpGs. We performed simple linear modeling to predict age from methylation level at each tRNA and each CpG.	501 502 503 504 505
<b>Data availability</b>	506
The MeDIP-seq data supporting the results of this article are available in the EMBL-EBI European Genome-phenome Archive (EGA) under Data set Accession number EGAD00010000983 ( <a href="https://www.ebi.ac.uk/ega/datasets/EGAD00010000983">https://www.ebi.ac.uk/ega/datasets/EGAD00010000983</a> ). The targeted BiS-sequencing data is available at: <a href="https://www.ncbi.nlm.nih.gov/bioproject/PRJNA635108">https://www.ncbi.nlm.nih.gov/bioproject/PRJNA635108</a>	507 508 509 510

## Code availability

511

Available at [https://github.com/RichardJActon/tRNA\\_paper\\_code](https://github.com/RichardJActon/tRNA_paper_code)

512

## Acknowledgements

513

We gratefully acknowledge the individuals from TwinsUK, Mavidos and the Hertfordshire cohort. TwinsUK received funding from the Wellcome Trust (Ref: 081878/Z/06/Z), European Community's Seventh Framework Programme (FP7/2007-2013), the National Institute for Health Research (NIHR)-funded BioResource, Clinical Research Facility and Biomedical Research Centre based at Guy's and St Thomas' NHS Foundation Trust in partnership with King's College London. Further funding support for the EpiTwin project was obtained from the European Research Council (project number 250157) and BGI. SNP Genotyping was performed by The Wellcome Trust Sanger Institute and National Eye Institute via NIH/CIDR. The authors would like to thank Nikki Graham for her assistance with the identification and pooling of the MAVIDOS and Hertfordshire DNA samples. The authors also acknowledge the use of the IRIDIS High Performance Computing Facility, and associated support services at the University of Southampton, in the completion of this work. The MRC-LEU is supported by the Medical Research Council (MRC). CGB received support from Diabetes UK (16/0005454). RJA was in receipt of a MRC Doctoral fund (1820097).

514

515

516

517

518

519

520

521

522

523

524

525

526

527

528

529

530

531

532

## Author Contributions

RJA designed experiments and analysed all the processed and experimental data. CGB conceived and designed the experiments. TDS, KW and JW conceived and provided TwinsUK MeDIP-seq data. YX, FG and JW produced raw MeDIP-seq data with WY and JB processing and quality controlling these data. WY contributed an analysis concept. CC, NH, ED, and KL provided MAVIDOS and Hertfordshire sample data. EB, EW, and CAM performed the targeted Bis sequencing experiment. PGH contributed additional data and discussion of results. RJA and CGB wrote the paper. All authors reviewed and approved the final manuscript.

## References

533

1. Partridge L, Deelen J, Slagboom PE. Facing up to the global challenges of ageing. *Nature*. Springer US; 2018;561: 45–56. doi:10.1038/s41586-018-0457-8 534  
535
2. Campisi J, Kapahi P, Lithgow GJ, Melov S, Newman JC, Verdin E. From discoveries in ageing research to therapeutics for healthy ageing. *Nature*. Springer US; 2019;571: 183–192. doi:10.1038/s41586-019-1365-2 536  
537
3. López-Otín C, Blasco MA, Partridge L, Serrano M, Kroemer G. The hallmarks of aging. *Cell*. 2013;153: 538  
1194–217. doi:10.1016/j.cell.2013.05.039 539
4. Booth LN, Brunet A. The Aging Epigenome. *Molecular Cell*. Elsevier Inc. 2016;62: 728–744. 540  
doi:10.1016/j.molcel.2016.05.013 541
5. Wilson VL, Jones PA. DNA methylation decreases in aging but not in immortal cells. *Science (New York, NY)*. 1983;220: 1055–7. Available: <http://www.ncbi.nlm.nih.gov/pubmed/6844925> 542  
543
6. Fraga MF, Ballestar E, Paz MF, Ropero S, Setien F, Ballestar ML, et al. From The Cover: Epigenetic differences arise during the lifetime of monozygotic twins. *Proceedings of the National Academy of Sciences*. 2005;102: 10604–10609. doi:10.1073/pnas.0500398102 544  
545
7. Chuong EB, Elde NC, Feschotte C. Regulatory activities of transposable elements: from conflicts to 546  
benefits. *Nature Reviews Genetics*. Nature Publishing Group; 2017;18: 71–86. doi:10.1038/nrg.2016.139 547  
548
8. Teschendorff AE, Menon U, Gentry-Maharaj A, Ramus SJ, Weisenberger DJ, Shen H, et al. 549  
Age-dependent DNA methylation of genes that are suppressed in stem cells is a hallmark of cancer. *Genome 550  
research*. 2010;20: 440–6. doi:10.1101/gr.103606.109 551
9. Rakyan VK, Down TA, Maslau S, Andrew T, Yang TP, Beyan H, et al. Human aging-associated DNA 552  
hypermethylation occurs preferentially at bivalent chromatin domains. *Genome Research*. 2010;20: 434–439. 553  
doi:10.1101/gr.103101.109 554
10. Hannum G, Guinney J, Zhao L, Zhang L, Hughes G, Sadda S, et al. Genome-wide methylation profiles 555  
reveal quantitative views of human aging rates. *Molecular cell*. Elsevier Inc. 2013;49: 359–367. 556  
doi:10.1016/j.molcel.2012.10.016 557
11. Horvath S. DNA methylation age of human tissues and cell types. *Genome biology*. 2013;14: R115. 558  
doi:10.1186/gb-2013-14-10-r115 559
12. Weidner CI, Lin Q, Koch CM, Eisele L, Beier F, Ziegler P, et al. Aging of blood can be tracked by DNA 560  
methylation changes at just three CpG sites. *Genome biology*. 2014;15: R24. doi:10.1186/gb-2014-15-2-r24 561
13. Bell CG, Lowe R, Adams PD, Baccarelli AA, Beck S, Bell JT, et al. DNA methylation aging clocks: 562  
challenges and recommendations. *Genome biology*. 2019;20: 249. doi:10.1186/s13059-019-1824-y 563

14. Horvath S, Raj K. DNA methylation-based biomarkers and the epigenetic clock theory of ageing. *Nature Reviews Genetics*. Springer US; 2018;19: 371–384. doi:10.1038/s41576-018-0004-3 564
15. Field AE, Robertson NA, Wang T, Havas A, Ideker T, Adams PD. DNA Methylation Clocks in Aging: Categories, Causes, and Consequences. *Molecular Cell*. Elsevier Inc. 2018;71: 882–895. 565  
doi:10.1016/j.molcel.2018.08.008 566
16. Bell CG, Xia Y, Yuan W, Gao F, Ward K, Roos L, et al. Novel regional age-associated DNA methylation changes within human common disease-associated loci. *Genome Biology*. 2016;17: 193. 569  
doi:10.1186/s13059-016-1051-8 570
17. Rideout EJ, Marshall L, Grewal SS. Drosophila RNA polymerase III repressor Maf1 controls body size and developmental timing by modulating tRNA<sup>iMet</sup> synthesis and systemic insulin signaling. *Proceedings of the National Academy of Sciences*. 2012;109: 1139–1144. doi:10.1073/pnas.1113311109 572  
573
18. Kolitz SE, Lorsch JR. Eukaryotic initiator tRNA: Finely tuned and ready for action. *FEBS Letters*. 575  
2010;584: 396–404. doi:10.1016/j.febslet.2009.11.047 576
19. Pavon-Eternod M, Gomes S, Rosner MR, Pan T. Overexpression of initiator methionine tRNA leads to global reprogramming of tRNA expression and increased proliferation in human epithelial cells. *RNA*. 2013;19: 577  
461–466. doi:10.1261/rna.037507.112 578
20. Eigen M, Lindemann B, Tietze M, Winkler-Oswatitsch R, Dress A, Haeseler A von. How old is the genetic code? Statistical geometry of tRNA provides an answer. *Science*. 1989;244: 673–679. doi:10.1126/science.2497522 580  
581
21. Tavernarakis N. Ageing and the regulation of protein synthesis: a balancing act? *Trends in Cell Biology*. 582  
2008;18: 228–235. doi:10.1016/j.tcb.2008.02.004 583
22. Pliatsika V, Loher P, Magee R, Telonis AG, Londin E, Shigematsu M, et al. MINTbase v2.0: a 584 comprehensive database for tRNA-derived fragments that includes nuclear and mitochondrial fragments from all 585 The Cancer Genome Atlas projects. *Nucleic Acids Research*. Oxford University Press; 2018;46: D152–D159. 586  
doi:10.1093/nar/gkx1075 587
23. Schimmel P. The emerging complexity of the tRNA world: mammalian tRNAs beyond protein synthesis. 588  
*Nature reviews Molecular cell biology*. Nature Publishing Group; 2018;19: 45–58. doi:10.1038/nrm.2017.77 589
24. Lee YS, Shibata Y, Malhotra A, Dutta A. A novel class of small RNAs: tRNA-derived RNA fragments (tRFs). *Genes & development*. 2009;23: 2639–49. doi:10.1101/gad.1837609 590  
591
25. Li S, Xu Z, Sheng J. tRNA-Derived Small RNA: A Novel Regulatory Small Non-Coding RNA. *Genes*. 592  
2018;9: 246. doi:10.3390/genes9050246 593
26. Xu W-L, Yang Y, Wang Y-D, Qu L-H, Zheng L-L. Computational Approaches to tRNA-Derived Small 594  
RNAs. *Non-Coding RNA*. 2017;3: 2. doi:10.3390/ncrna3010002 595

27. Chan PP, Lowe TM. GtRNAdb: a database of transfer RNA genes detected in genomic sequence. Nucleic acids research. 2009;37: D93–7. doi:10.1093/nar/gkn787 596
28. Parisien M, Wang X, Pan T. Diversity of human tRNA genes from the 1000-genomes project. RNA Biology. 2013;10: 1853–1867. doi:10.4161/rna.27361 598
29. Lodish H, Berk A, Zipursky SL, Matsudaira P, Baltimore D, Darnell J. Molecular Cell Biology, 4th edition [Internet]. 4th ed. New York: W. H. Freeman; 2000. Available: 600  
<https://www.ncbi.nlm.nih.gov/books/NBK21475/> 602
30. Schramm L. Recruitment of RNA polymerase III to its target promoters. Genes & Development. 2002;16: 603  
2593–2620. doi:10.1101/gad.1018902 604
31. Canella D, Praz V, Reina JH, Cousin P, Hernandez N. Defining the RNA polymerase III transcriptome: 605  
Genome-wide localization of the RNA polymerase III transcription machinery in human cells. Genome research. 606  
2010;20: 710–21. doi:10.1101/gr.101337.109 607
32. Besser D, Götz F, Schulze-Forster K, Wagner H, Kröger H, Simon D. DNA methylation inhibits 608  
transcription by RNA polymerase III of a tRNA gene, but not of a 5S rRNA gene. FEBS letters. 1990;269: 609  
358–62. doi:10.1016/0014-5793(90)81193-R 610
33. Varshney D, Vavrova-Anderson J, Oler AJ, Cowling VH, Cairns BR, White RJ. SINE transcription by 611  
RNA polymerase III is suppressed by histone methylation but not by DNA methylation. Nature communications. 612  
Nature Publishing Group; 2015;6: 6569. doi:10.1038/ncomms7569 613
34. Murawski M, Szczesniak B, Zoladek T, Hopper AK, Martin NC, Boguta M. maf1 mutation alters the 614  
subcellular localization of the Mod5 protein in yeast. Acta biochimica Polonica. 1994;41: 441–8. Available:  
<http://www.ncbi.nlm.nih.gov/pubmed/7732762> 616
35. Pluta K, Lefebvre O, Martin NC, Smagowicz WJ, Stanford DR, Ellis SR, et al. Maf1p, a Negative 617  
Effector of RNA Polymerase III in *Saccharomyces cerevisiae*. Molecular and Cellular Biology. 2001;21: 618  
5031–5040. doi:10.1128/MCB.21.15.5031-5040.2001 619
36. Mange F, Praz V, Migliavacca E, Willis IM, Schütz F, Hernandez N. Diurnal regulation of RNA 620  
polymerase III transcription is under the control of both the feeding–fasting response and the circadian clock. 621  
Genome Research. 2017;27: 973–984. doi:10.1101/gr.217521.116 622
37. Kennedy BK, Lamming DW. The Mechanistic Target of Rapamycin: The Grand ConducTOR of 623  
Metabolism and Aging. Cell Metabolism. Elsevier Inc. 2016;23: 990–1003. doi:10.1016/j.cmet.2016.05.009 624
38. Nwanaji-Enwerem JC, Weisskopf MG, Baccarelli AA. Multi-tissue DNA methylation age: Molecular 625  
relationships and perspectives for advancing biomarker utility. Ageing Research Reviews. Elsevier; 2018;45: 626  
15–23. doi:10.1016/j.arr.2018.04.005 627

39. Hansen M, Taubert S, Crawford D, Libina N, Lee S-J, Kenyon C. Lifespan extension by conditions that inhibit translation in *Caenorhabditis elegans*. *Aging Cell*. 2007;6: 95–110. doi:10.1111/j.1474-9726.2006.00267.x 628
40. Filer D, Thompson MA, Takhaviev V, Dobson AJ, Kotronaki I, Green JWM, et al. RNA polymerase III limits longevity downstream of TORC1. *Nature*. Nature Publishing Group; 2017;552: 263–267. 629  
doi:10.1038/nature25007 630
41. Dahabi JM, Spindler SR, Atamna H, Yamakawa A, Boffelli D, Mote P, et al. 5' tRNA halves are present 631 as abundant complexes in serum, concentrated in blood cells, and modulated by aging and calorie restriction. 632  
*BMC Genomics*. 2013;14: 298. doi:10.1186/1471-2164-14-298 633
42. Zhou W, Laird PW, Shen H. Comprehensive characterization, annotation and innovative use of Infinium 634 DNA methylation BeadChip probes. *Nucleic Acids Research*. 2016;45: gkw967. doi:10.1093/nar/gkw967 635
43. Van Bortle K, Phanstiel DH, Snyder MP. Topological organization and dynamic regulation of human 636 tRNA genes during macrophage differentiation. *Genome Biology*. *Genome Biology*; 2017;18: 180. 637  
doi:10.1186/s13059-017-1310-3 638
44. Down TA, Rakyan VK, Turner DJ, Flicek P, Li H, Kulesha E, et al. A Bayesian deconvolution strategy 639 for immunoprecipitation-based DNA methylome analysis. *Nature Biotechnology*. 2008;26: 779–785. 640  
doi:10.1038/nbt1414 641
45. Lowe TM, Chan PP. tRNAscan-SE On-line: integrating search and context for analysis of transfer RNA 642 genes. *Nucleic Acids Research*. 2016;44: W54–W57. doi:10.1093/nar/gkw413 643
46. Amemiya HM, Kundaje A, Boyle AP. The ENCODE Blacklist: Identification of Problematic Regions of 644 the Genome. *Scientific Reports*. 2019;9: 9354. doi:10.1038/s41598-019-45839-z 645
47. Geiger H, Haan G de, Florian MC. The ageing haematopoietic stem cell compartment. *Nature Reviews 646 Immunology*. Nature Publishing Group; 2013;13: 376–389. doi:10.1038/nri3433 647
48. Ziller MJ, Gu H, Müller F, Donaghey J, Tsai LT-Y, Kohlbacher O, et al. Charting a dynamic DNA 648 methylation landscape of the human genome. *Nature*. 2013;500: 477–81. doi:10.1038/nature12433 649
49. Christensen BC, Houseman EA, Marsit CJ, Zheng S, Wrensch MR, Wiemels JL, et al. Aging and 650 Environmental Exposures Alter Tissue-Specific DNA Methylation Dependent upon CpG Island Context. 651 Schübeler D, editor. *PLoS Genetics*. 2009;5: e1000602. doi:10.1371/journal.pgen.1000602 652
50. Heyn H, Li N, Ferreira HJ, Moran S, Pisano DG, Gomez A, et al. Distinct DNA methylomes of newborns 653 and centenarians. *Proceedings of the National Academy of Sciences*. 2012;109: 10522–10527. 654  
doi:10.1073/pnas.1120658109 655
51. Houseman EA, Accomando WP, Koestler DC, Christensen BC, Marsit CJ, Nelson HH, et al. DNA 656 methylation arrays as surrogate measures of cell mixture distribution. *BMC Bioinformatics*. 2012;13: 86. 657  
doi:10.1186/1471-2105-13-86 658
52. Houseman EA, Accomando WP, Koestler DC, Christensen BC, Marsit CJ, Nelson HH, et al. DNA 659 methylation arrays as surrogate measures of cell mixture distribution. *BMC Bioinformatics*. 2012;13: 86. 660  
doi:10.1186/1471-2105-13-86 661

doi:10.1186/1471-2105-13-86

- 660  
52. Müller F, Scherer M, Assenov Y, Lutsik P, Walter J, Lengauer T, et al. RnBeads 2.0: comprehensive  
661 analysis of DNA methylation data. *Genome Biology*. *Genome Biology*; 2019;20: 55.  
662  
doi:10.1186/s13059-019-1664-9  
663  
53. Meuleman W. Epilogos [Internet]. 2019. Available:  
664 <https://epilogos.altius.org/>  
665  
54. Ernst J, Kheradpour P, Mikkelsen TS, Shoresh N, Ward LD, Epstein CB, et al. Mapping and analysis of  
666 chromatin state dynamics in nine human cell types. *Nature*. 2011;473: 43–49. doi:10.1038/nature09906  
667  
55. Reinius LE, Acevedo N, Joerink M, Pershagen G, Dahlén S-E, Greco D, et al. Differential DNA  
668 Methylation in Purified Human Blood Cells: Implications for Cell Lineage and Studies on Disease Susceptibility.  
669 Ting AH, editor. *PLoS ONE*. 2012;7: e41361. doi:10.1371/journal.pone.0041361  
670  
56. Gu Z, Eils R, Schlesner M. Complex heatmaps reveal patterns and correlations in multidimensional  
671 genomic data. *Bioinformatics*. 2016;32: 2847–2849. doi:10.1093/bioinformatics/btw313  
672  
57. Schmitt BM, Rudolph KLM, Karagianni P, Fonseca NA, White RJ, Talianidis I, et al. High-resolution  
673 mapping of transcriptional dynamics across tissue development reveals a stable mRNA–tRNA interface. *Genome*  
674 *Research*. 2014;24: 1797–1807. doi:10.1101/gr.176784.114  
675  
58. Dittmar KA, Goodenbour JM, Pan T. Tissue-specific differences in human transfer RNA expression.  
676 PLoS genetics. 2006;2: e221. doi:10.1371/journal.pgen.0020221  
677  
59. Sagi D, Rak R, Gingold H, Adir I, Maayan G, Dahan O, et al. Tissue- and Time-Specific Expression of  
678 Otherwise Identical tRNA Genes. Chisholm AD, editor. *PLOS Genetics*. 2016;12: e1006264.  
679  
doi:10.1371/journal.pgen.1006264  
680  
60. Slieker RC, Iterson M van, Luijk R, Beekman M, Zhernakova DV, Moed MH, et al. Age-related accrual of  
681 methylomic variability is linked to fundamental ageing mechanisms. *Genome biology*. *Genome Biology*; 2016;17:  
682 191. doi:10.1186/s13059-016-1053-6  
683  
61. Yang Z, Wong A, Kuh D, Paul DS, Rakyan VK, Leslie RD, et al. Correlation of an epigenetic mitotic  
684 clock with cancer risk. *Genome Biology*. *Genome Biology*; 2016;17: 205. doi:10.1186/s13059-016-1064-3  
685  
62. Nazor KL, Altun G, Lynch C, Tran H, Harness JV, Slavin I, et al. Recurrent Variations in DNA  
686 Methylation in Human Pluripotent Stem Cells and Their Differentiated Derivatives. *Cell Stem Cell*. 2012;10:  
687 620–634. doi:10.1016/j.stem.2012.02.013  
688  
63. Petkovich DA, Podolskiy DI, Lobanov AV, Lee S-G, Miller RA, Gladyshev VN. Using DNA Methylation  
689 Profiling to Evaluate Biological Age and Longevity Interventions. *Cell Metabolism*. 2017;25: 954–960.e6.  
690  
doi:10.1016/j.cmet.2017.03.016  
691

64. Thornlow BP, Armstrong J, Holmes AD, Howard JM, Corbett-Detig RB, Lowe TM. Predicting transfer RNA gene activity from sequence and genome context. *Genome Research*. 2020;30: 85–94. doi:10.1101/gr.256164.119
65. Ehrlich M. DNA hypermethylation in disease: mechanisms and clinical relevance. *Epigenetics*. Taylor & Francis; 2019;14: 1141–1163. doi:10.1080/15592294.2019.1638701
66. Xu Z, Taylor JA. Genome-wide age-related DNA methylation changes in blood and other tissues relate to histone modification, expression and cancer. *Carcinogenesis*. 2014;35: 356–364. doi:10.1093/carcin/bgt391
67. Slieker RC, Relton CL, Gaunt TR, Slagboom PE, Heijmans BT. Age-related DNA methylation changes are tissue-specific with ELOVL2 promoter methylation as exception. *Epigenetics and Chromatin*. BioMed Central; 2018;11: 1–11. doi:10.1186/s13072-018-0191-3
68. Zhu T, Zheng SC, Paul DS, Horvath S, Teschendorff AE. Cell and tissue type independent age-associated DNA methylation changes are not rare but common. *Aging*. 2018;10: 3541–3557. doi:10.18632/aging.101666
69. Lappalainen T, Greally JM. Associating cellular epigenetic models with human phenotypes. *Nature Reviews Genetics*. Nature Publishing Group; 2017;18: 441–451. doi:10.1038/nrg.2017.32
70. Moskowitz DM, Zhang DW, Hu B, Le Saux S, Yanes RE, Ye Z, et al. Epigenomics of human CD8 T cell differentiation and aging. *Science Immunology*. 2017;2: eaag0192. doi:10.1126/sciimmunol.aag0192
71. Hashimoto K, Kouno T, Ikawa T, Hayatsu N, Miyajima Y, Yabukami H, et al. Single-cell transcriptomics reveals expansion of cytotoxic CD4 T cells in supercentenarians. *Proceedings of the National Academy of Sciences of the United States of America*. 2019;116: 24242–24251. doi:10.1073/pnas.1907883116
72. Goodenbour JM, Pan T. Diversity of tRNA genes in eukaryotes. *Nucleic acids research*. 2006;34: 6137–46. doi:10.1093/nar/gkl725
73. Keam SP, Young PE, McCorkindale AL, Dang THY, Clancy JL, Humphreys DT, et al. The human Piwi protein Hiwi2 associates with tRNA-derived piRNAs in somatic cells. *Nucleic Acids Research*. 2014;42: 8984–8995. doi:10.1093/nar/gku620
74. Geslain R, Pan T. Functional Analysis of Human tRNA Isodecoders. *Journal of Molecular Biology*. 2010;396: 821–831. doi:10.1016/j.jmb.2009.12.018
75. Kirchner S, Cai Z, Rauscher R, Kastelic N, Anding M, Czech A, et al. Alteration of protein function by a silent polymorphism linked to tRNA abundance. Hurst L, editor. *PLOS Biology*. 2017;15: e2000779. doi:10.1371/journal.pbio.2000779
76. Li S, Shi X, Chen M, Xu N, Sun D, Bai R, et al. Angiogenin promotes colorectal cancer metastasis via tiRNA production. *International Journal of Cancer*. 2019; ijc.32245. doi:10.1002/ijc.32245
77. Kim HK, Fuchs G, Wang S, Wei W, Zhang Y, Park H, et al. A transfer-RNA-derived small RNA

- regulates ribosome biogenesis. *Nature*. Nature Publishing Group; 2017;552: 57–62. doi:10.1038/nature25005 724
78. Martinez G, Choudury SG, Slotkin RK. tRNA-derived small RNAs target transposable element 725 transcripts. *Nucleic Acids Research*. 2017;45: 5142–5152. doi:10.1093/nar/gkx103 726
79. Torres AG, Reina O, Stephan-Otto Attolini C, Ribas de Pouplana L. Differential expression of human 727 tRNA genes drives the abundance of tRNA-derived fragments. *Proceedings of the National Academy of Sciences*. 728 2019;116: 201821120. doi:10.1073/pnas.1821120116 729
80. Gu P, Jia S, Takasugi T, Smith E, Nandakumar J, Hendrickson E, et al. CTC1-STN1 coordinates G- and 730 C-strand synthesis to regulate telomere length. *Aging Cell*. 2018;17: e12783. doi:10.1111/acel.12783 731
81. Wang Y, Brady KS, Caiello BP, Ackerson SM, Stewart JA. Human CST suppresses origin licensing and 732 promotes AND-1/Ctf4 chromatin association. *Life Science Alliance*. 2019;2: e201800270. 733  
doi:10.26508/lسا.201800270 734
82. Sargolzaeiaval F, Zhang J, Schleit J, Lessel D, Kubisch C, Precioso DR, et al. CTC1 mutations in a 735 Brazilian family with progeroid features and recurrent bone fractures. *Molecular Genetics & Genomic Medicine*. 736 2018;6: 1148–1156. doi:10.1002/mgg3.495 737
83. Gomez-Roman N, Grandori C, Eisenman RN, White RJ. Direct activation of RNA polymerase III 738 transcription by c-Myc. *Nature*. 2003;421: 290–294. doi:10.1038/nature01327 739
84. Crighton D. p53 represses RNA polymerase III transcription by targeting TBP and inhibiting promoter 740 occupancy by TFIIIB. *The EMBO Journal*. 2003;22: 2810–2820. doi:10.1093/emboj/cdg265 741
85. Sutcliffe JE, Brown TRP, Allison SJ, Scott PH, White RJ. Retinoblastoma Protein Disrupts Interactions 742 Required for RNA Polymerase III Transcription. *Molecular and Cellular Biology*. 2000;20: 9192–9202. 743  
doi:10.1128/MCB.20.24.9192-9202.2000 744
86. Schmitt BM, Rudolph KLM, Karagianni P, Fonseca NA, White RJ, Talianidis I, et al. High-resolution 745 mapping of transcriptional dynamics across tissue development reveals a stable mRNA-tRNA interface. *Genome* 746 research. 2014;24: 1797–807. doi:10.1101/gr.176784.114 747
87. Gerber A, Ito K, Chu C-S, Roeder RG. Gene-Specific Control of tRNA Expression by RNA Polymerase II. 748 *Molecular Cell*. Elsevier Inc. 2020;78: 765–778.e7. doi:10.1016/j.molcel.2020.03.023 749
88. Gingold H, Tehler D, Christoffersen NR, Nielsen MM, Asmar F, Kooistra SM, et al. A Dual Program for 750 Translation Regulation in Cellular Proliferation and Differentiation. *Cell*. Elsevier Inc. 2014;158: 1281–1292. 751  
doi:10.1016/j.cell.2014.08.011 752
89. Rudolph KLM, Schmitt BM, Villar D, White RJ, Marioni JC, Kutter C, et al. Codon-Driven 753 Translational Efficiency Is Stable across Diverse Mammalian Cell States. Galtier N, editor. *PLoS genetics*. 754 2016;12: e1006024. doi:10.1371/journal.pgen.1006024 755

90. Gingold H, Dahan O, Pilpel Y. Dynamic changes in translational efficiency are deduced from codon usage of the transcriptome. *Nucleic acids research*. 2012;40: 10053–63. doi:10.1093/nar/gks772 756
91. Thornlow BP, Hough J, Roger JM, Gong H, Lowe TM, Corbett-Detig RB. Transfer RNA genes experience exceptionally elevated mutation rates. *Proceedings of the National Academy of Sciences*. 2018;115: 758  
8996–9001. doi:10.1073/pnas.1801240115 759  
760
92. Iben JR, Maraia RJ. tRNA gene copy number variation in humans. *Gene*. 2014;536: 376–384. 761  
doi:10.1016/j.gene.2013.11.049 762
93. Darrow EM, Chadwick BP. A novel tRNA variable number tandem repeat at human chromosome 1q23.3 763  
is implicated as a boundary element based on conservation of a CTCF motif in mouse. *Nucleic Acids Research*. 764  
2014;42: 6421–6435. doi:10.1093/nar/gku280 765
94. Huang S-q, Sun B, Xiong Z-p, Shu Y, Zhou H-h, Zhang W, et al. The dysregulation of tRNAs and tRNA 766  
derivatives in cancer. *Journal of Experimental & Clinical Cancer Research. Journal of Experimental & Clinical* 767  
*Cancer Research*; 2018;37: 101. doi:10.1186/s13046-018-0745-z 768
95. Krishnan P, Ghosh S, Wang B, Heyns M, Li D, Mackey JR, et al. Genome-wide profiling of transfer 769  
RNAs and their role as novel prognostic markers for breast cancer. *Scientific Reports*. Nature Publishing Group; 770  
2016;6: 32843. doi:10.1038/srep32843 771
96. Müller CA, Nieduszynski CA. DNA replication timing influences gene expression level. *The Journal of* 772  
*Cell Biology*. 2017;216: 1907–1914. doi:10.1083/jcb.201701061 773
97. Du Q, Bert SA, Armstrong NJ, Caldon CE, Song JZ, Nair SS, et al. Replication timing and epigenome 774  
remodelling are associated with the nature of chromosomal rearrangements in cancer. *Nature Communications*. 775  
Springer US; 2019;10: 416. doi:10.1038/s41467-019-08302-1 776
98. Cruickshanks HA, McBryan T, Nelson DM, VanderKraats ND, Shah PP, Tuyn J van, et al. Senescent 777  
cells harbour features of the cancer epigenome. *Nature Cell Biology*. 2013;15: 1495–1506. doi:10.1038/ncb2879 778
99. Raab JR, Chiu J, Zhu J, Katzman S, Kurukuti S, Wade PA, et al. Human tRNA genes function as 779  
chromatin insulators. *The EMBO journal*. Nature Publishing Group; 2012;31: 330–50. 780  
doi:10.1038/emboj.2011.406 781
100. Noma K-i, Cam HP, Maraia RJ, Grewal SIS. A role for TFIIIC transcription factor complex in genome 782  
organization. *Cell*. 2006;125: 859–72. doi:10.1016/j.cell.2006.04.028 783
101. Sun L, Yu R, Dang W. Chromatin Architectural Changes during Cellular Senescence and Aging. *Genes*. 784  
2018;9: 211. doi:10.3390/genes9040211 785
102. Moayyeri A, Hammond CJ, Valdes AM, Spector TD. Cohort Profile: TwinsUK and Healthy Ageing 786  
Twin Study. *International Journal of Epidemiology*. 2013;42: 76–85. doi:10.1093/ije/dyr207 787

103. Harvey NC, Javaid K, Bishop N, Kennedy S, Papageorghiou AT, Fraser R, et al. MAVIDOS Maternal Vitamin D Osteoporosis Study: study protocol for a randomized controlled trial. The MAVIDOS Study Group. Trials. 2012;13: 13. doi:10.1186/1745-6215-13-13
104. Syddall H, Aihie Sayer A, Dennison E, Martin H, Barker D, Cooper C. Cohort Profile: The Hertfordshire Cohort Study. International Journal of Epidemiology. 2005;34: 1234–1242. doi:10.1093/ije/dyi127
105. Quinlan AR, Hall IM. BEDTools: a flexible suite of utilities for comparing genomic features. Bioinformatics. University of Utah; 2010;26: 841–842. doi:10.1093/bioinformatics/btq033
106. Bell CG, Gao F, Yuan W, Roos L, Acton RJ, Xia Y, et al. Obligatory and facilitative allelic variation in the DNA methylome within common disease-associated loci. Nature Communications. 2018;9: 8. doi:10.1038/s41467-017-01586-1
107. Lienhard M, Grimm C, Morkel M, Herwig R, Chavez L. MEDIPS: genome-wide differential coverage analysis of sequencing data derived from DNA enrichment experiments. Bioinformatics. 2014;30: 284–286. doi:10.1093/bioinformatics/btt650
108. Bell CG, Wilson GA, Butcher LM, Roos C, Walter L, Beck S. Human-specific CpG "beacons" identify loci associated with human-specific traits and disease. Epigenetics. 2012;7: 1188–99. doi:10.4161/epi.22127
109. North BV, Curtis D, Sham PC. A Note on the Calculation of Empirical P Values from Monte Carlo Procedures. The American Journal of Human Genetics. 2003;72: 498–499. doi:10.1086/346173
110. Li L-C, Dahiya R. MethPrimer: designing primers for methylation PCRs. Bioinformatics (Oxford, England). 2002;18: 1427–31. Available: <http://www.ncbi.nlm.nih.gov/pubmed/12424112>
111. Andrews S. FastQC [Internet]. Cambridge: Babraham Bioinformatics; 2010. Available: <http://www.bioinformatics.babraham.ac.uk/projects/fastqc>
112. Ewels P, Magnusson M, Lundin S, Käller M. MultiQC: summarize analysis results for multiple tools and samples in a single report. Bioinformatics (Oxford, England). 2016;32: 3047–8. doi:10.1093/bioinformatics/btw354
113. Martin M. Cutadapt removes adapter sequences from high-throughput sequencing reads. EMBnetjournal. 2011;17: 10. doi:10.14806/ej.17.1.200
114. Krueger F. Trim Galore [Internet]. 2015. Available: [https://www.bioinformatics.babraham.ac.uk/projects/trim%7B/\\_%7Dgalore/](https://www.bioinformatics.babraham.ac.uk/projects/trim%7B/_%7Dgalore/)
115. Krueger F, Andrews SR. Bismark: a flexible aligner and methylation caller for Bisulfite-Seq applications. Bioinformatics. 2011;27: 1571–1572. doi:10.1093/bioinformatics/btr167
116. Langmead B, Salzberg SL. Fast gapped-read alignment with Bowtie 2. Nature methods. 2012;9: 357–9. doi:10.1038/nmeth.1923

117. Ritchie ME, Phipson B, Wu D, Hu Y, Law CW, Shi W, et al. limma powers differential expression analyses for RNA-sequencing and microarray studies. *Nucleic Acids Research*. 2015;43: e47–e47. doi:10.1093/nar/gkv007
118. Sean D, Meltzer PS. GEOquery: A bridge between the Gene Expression Omnibus (GEO) and BioConductor. *Bioinformatics*. 2007;23: 1846–1847. doi:10.1093/bioinformatics/btm254
119. Grossman RL, Heath AP, Ferretti V, Varmus HE, Lowy DR, Kibbe WA, et al. Toward a Shared Vision for Cancer Genomic Data. *New England Journal of Medicine*. 2016;375: 1109–1112. doi:10.1056/NEJMmp1607591
120. Derrien T, Estellé J, Marco Sola S, Knowles DG, Raineri E, Guigó R, et al. Fast Computation and Applications of Genome Mappability. Ouzounis CA, editor. *PLoS ONE*. 2012;7: e30377. doi:10.1371/journal.pone.0030377

# Supplementary materials

830

## Supplementary Figures

831

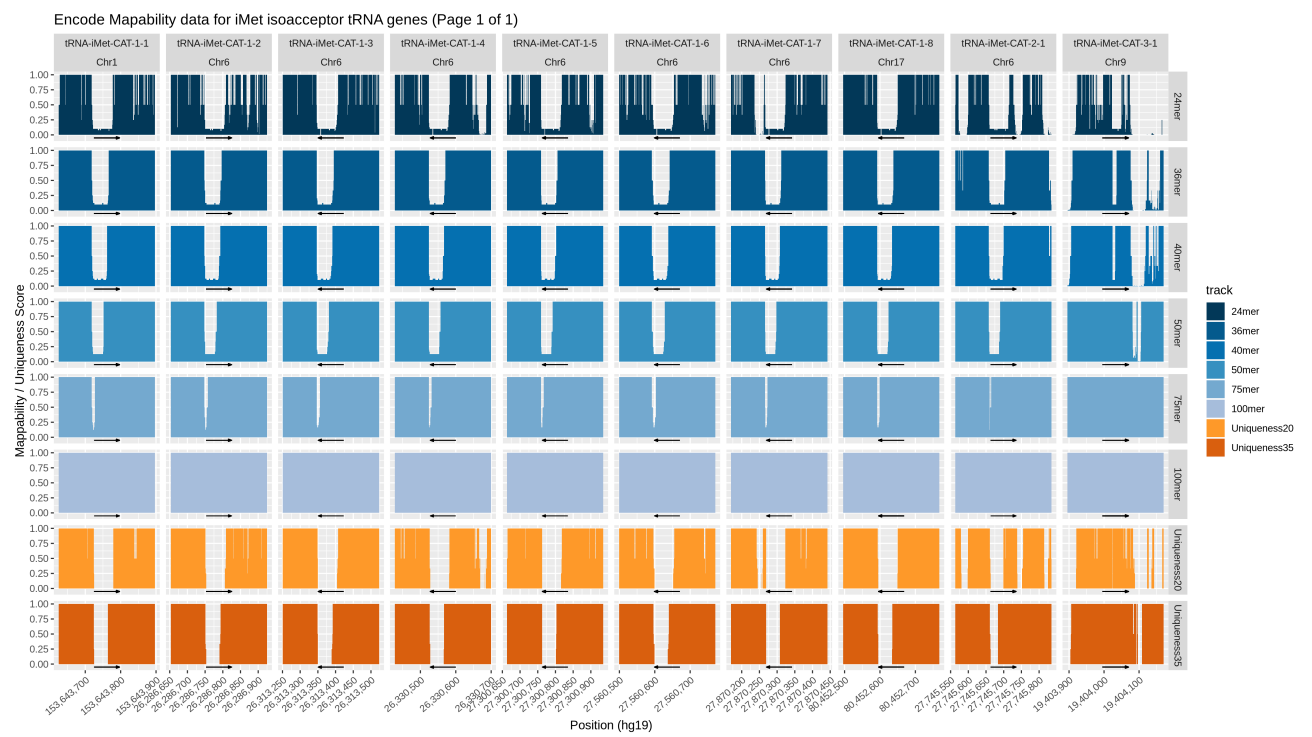


**Fig S1.** Example of mappability data from the encode mappability tracks [120] for the initiator methionine tRNA genes.

## tRNA mappability

tRNA region only Vs tRNA +/- 500bp

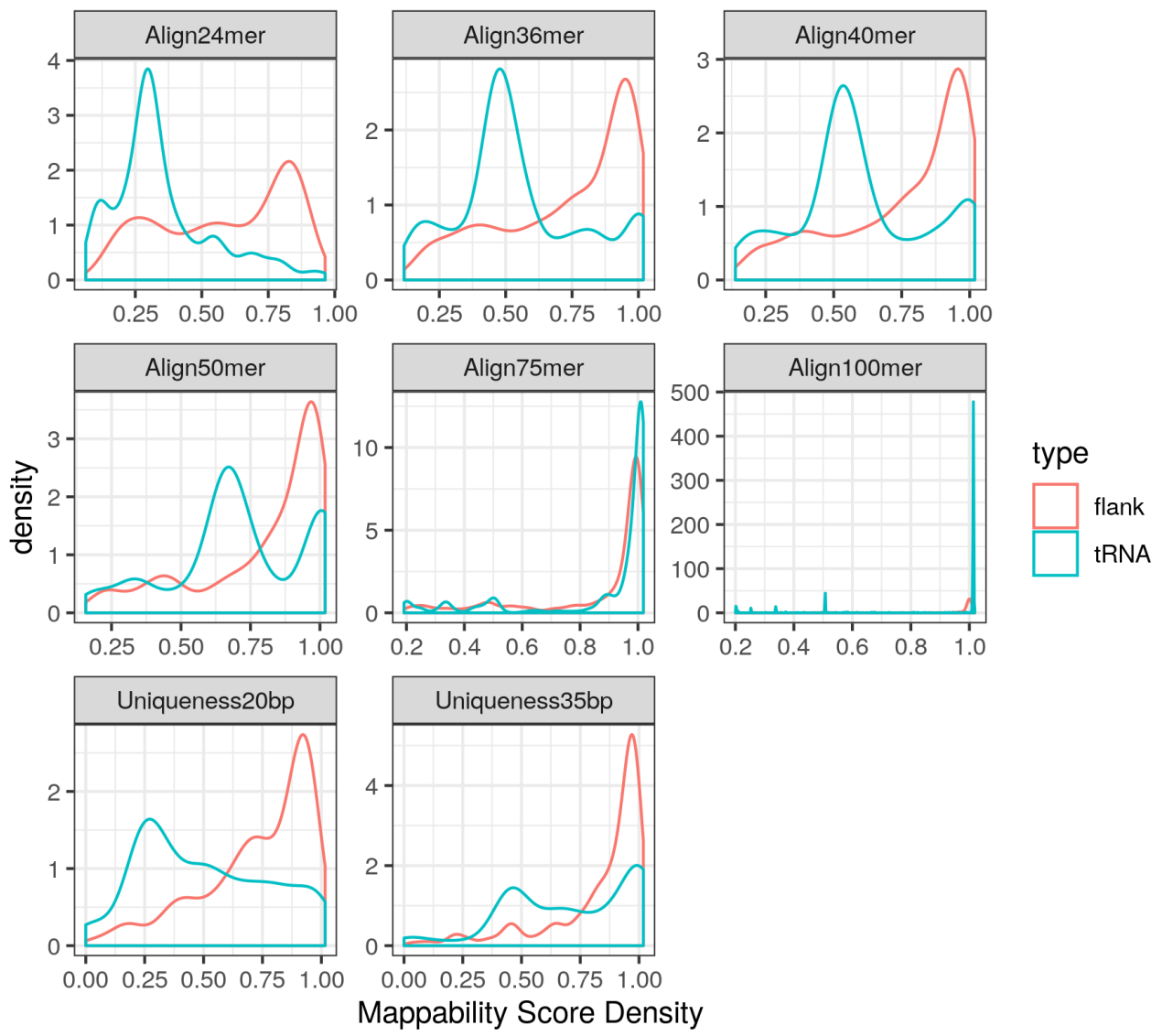


**Fig S2.** Mappability score density of the tRNA genes increases with read length and is greater when flanking regions ( $\pm 500\text{bp}$ ) are included. Mappability score density is computed as the area under the encode mappability tracks [120] over the length of the region.

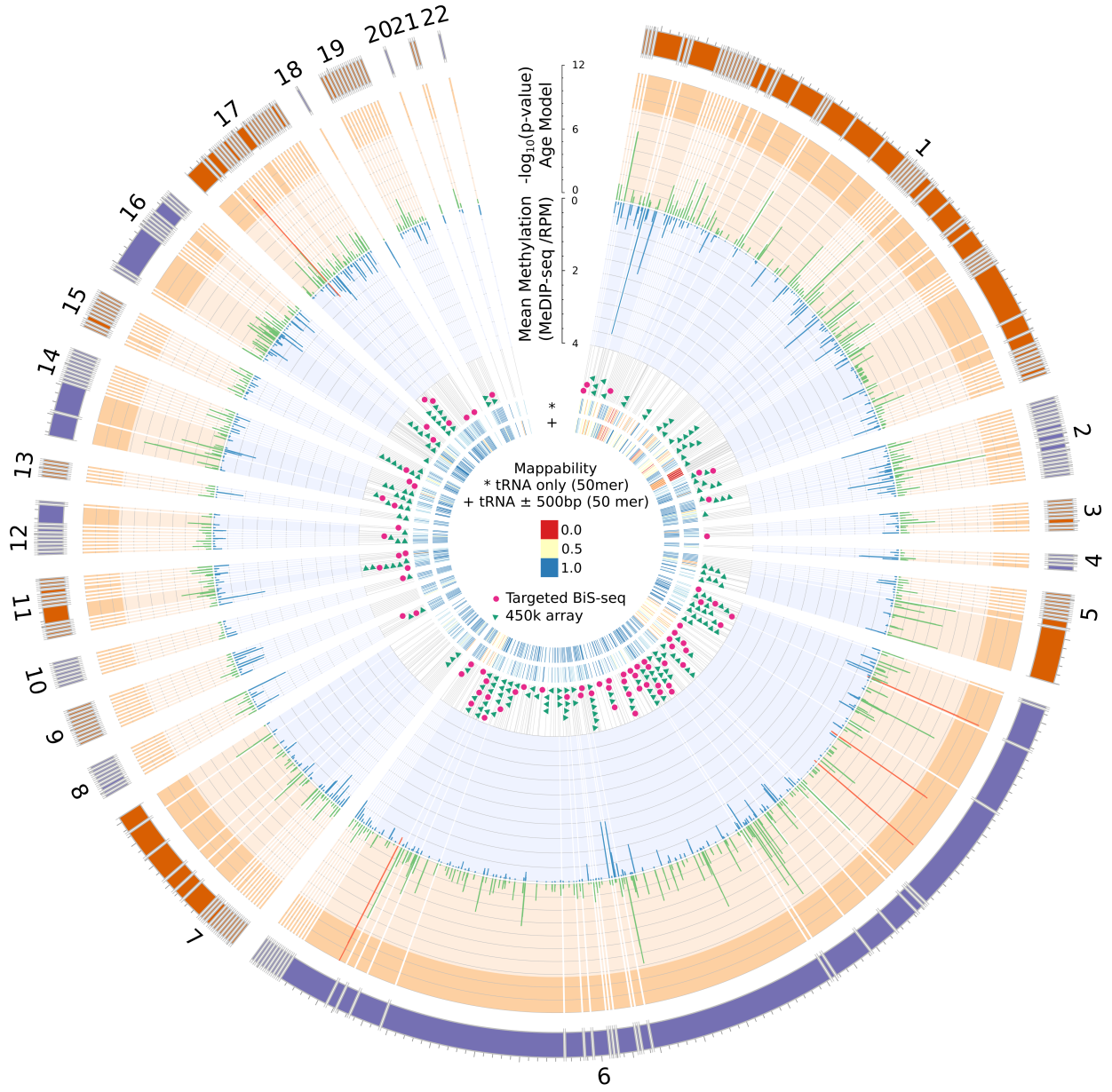


**Fig S3.** Human tRNA genes overview. From the outside in: Chromosome ideograms scaled by the number of tRNA genes (total = 598), as excludes chromosome X (10), Y (0) and contig chr1\_g1000192\_random (2; see Methods). tRNA genes within 20kbp of one another are grouped with breaks inserted between these clusters. Radial grey lines represent the location of tRNA genes in the genome.  $-\log_{10}(p\text{-value})$  for the blood cell-type and batch corrected age model are shown for each window overlapping a tRNA gene in green. Mean methylation across all samples ( $n=3001$ ) in RPM (reads per million base pairs) is shown in blue. Genome-wide significant cell-type & batch corrected ( $p < 4.34 \times 10^{-9}$ ) tRNAs show in red. The 158 Loci covered by 213 probes on the 450k array which directly overlap a tRNA gene are shown with green triangles. The 84 loci targeted for bisulfite sequencing in this study are indicated in magenta. Mappability score density is computed as the area under the encode mappability tracks [120] over the length of the region.

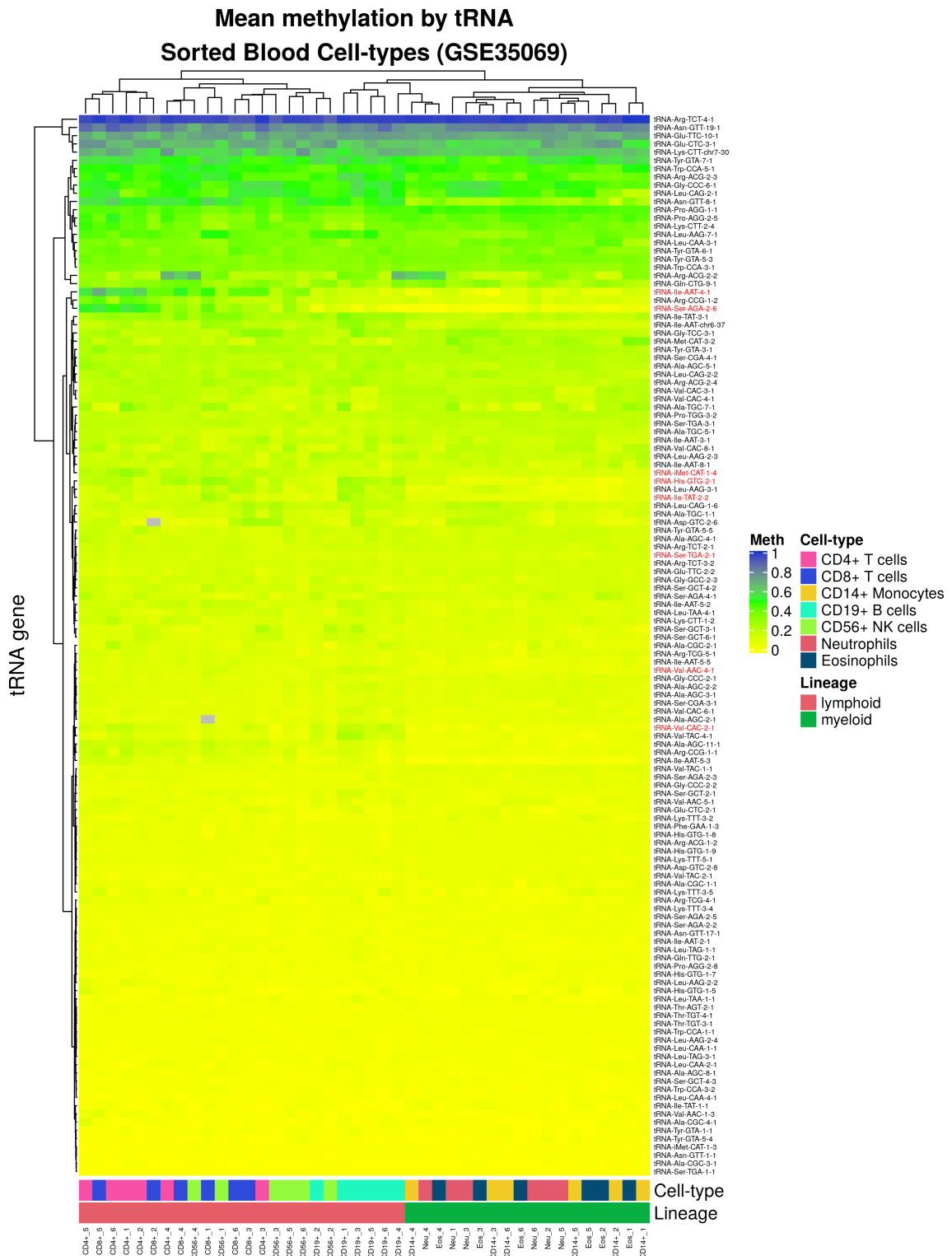


**Fig S4.** Heatmap Mean Methylation of probes covering each tRNA in 7 cell-type fractions from 6 Male individuals. Showing all 150 tRNAs covered by 213 probes on the Illumina 450k array. Data from GSE35069 [55] downloaded using GEOquery [56,118].

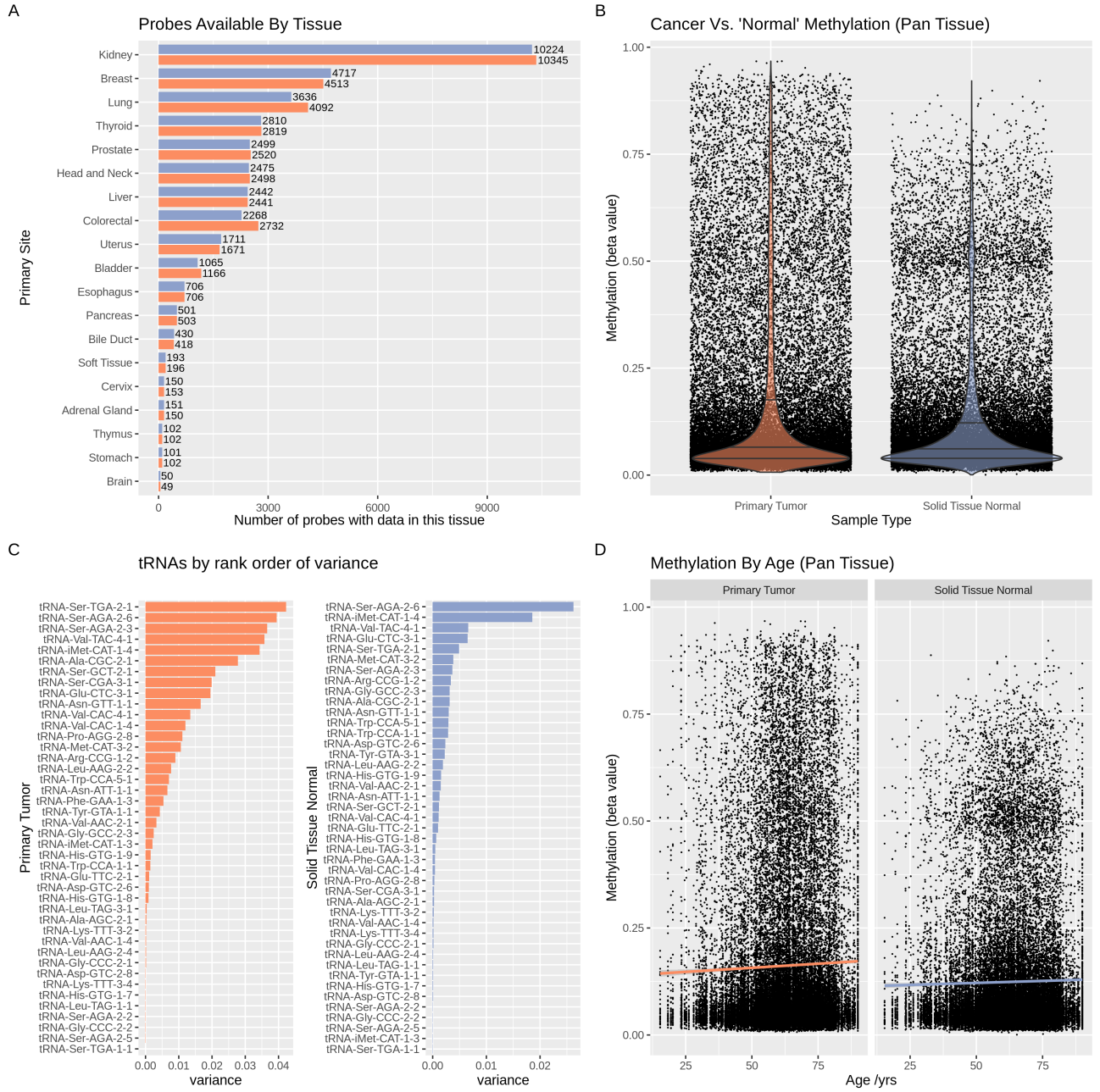


**Fig S5.** Global properties of tRNA methylation data for 45 tRNA genes across 19 tissues with matched normal and tumour samples from 733 cases in TCGA [61,62].

## Mean methylation by tRNA In Solid Tissue Normal Samples

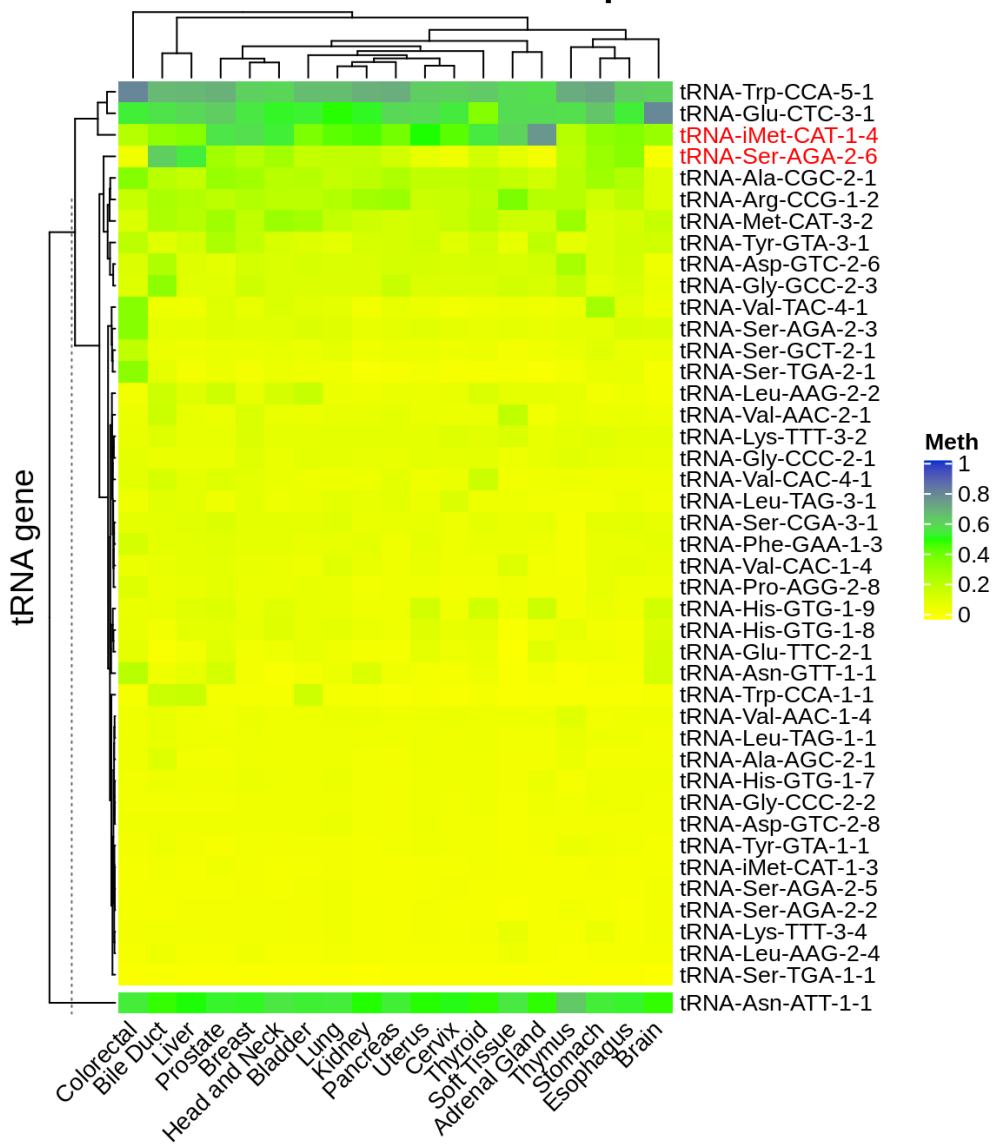


**Fig S6.** Mean Methylation of 43 tRNAs in 19 tissues. Possible pseudogene (tRNA-Asn-ATT-1-1) is shown in a separate cluster beneath the main heatmap [56].

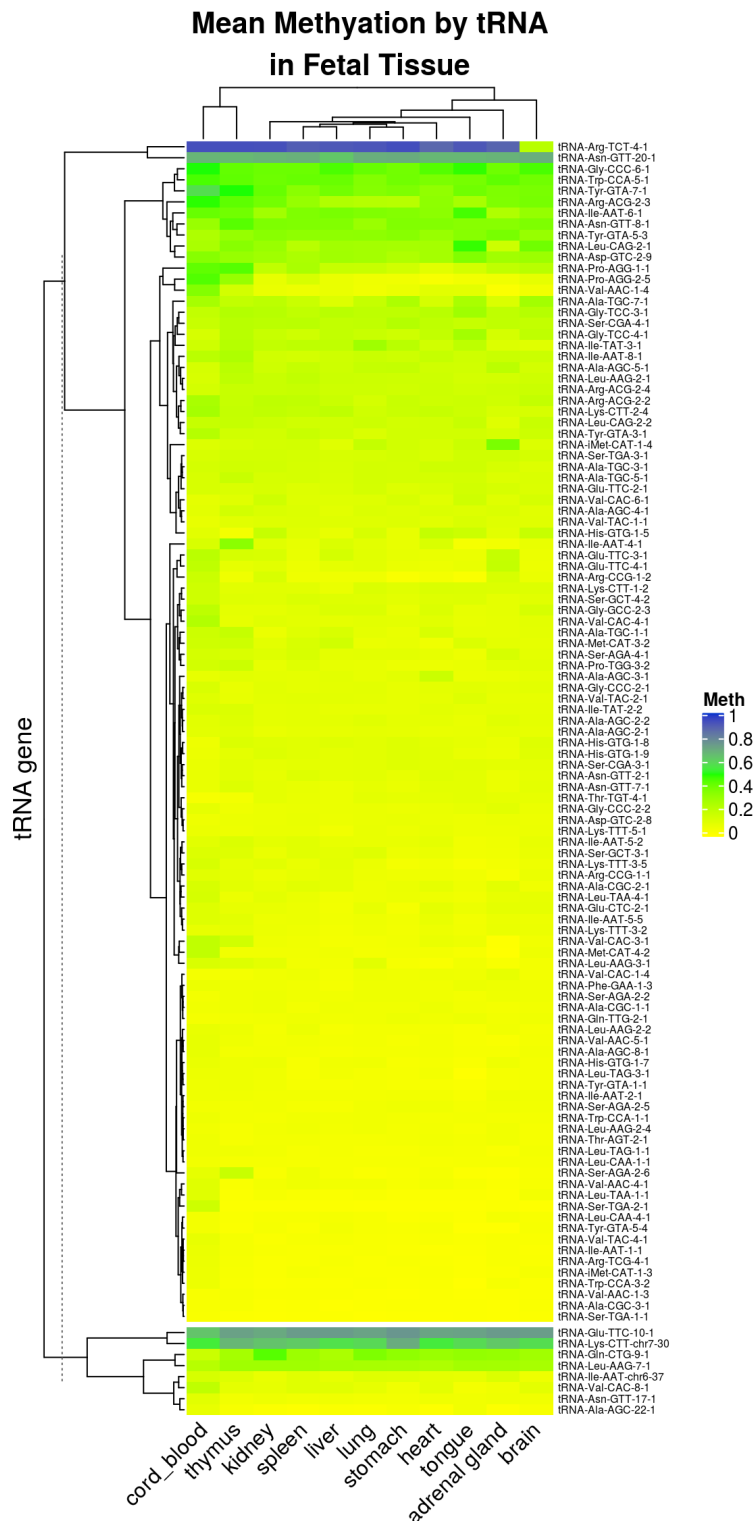


**Fig S7.** Mean Methylation of 115 tRNAs in 11 tissues. Possible pseudogenes are shown in a separate cluster beneath the main heatmap [56].

## CpG Density in tRNA Regions

Compared to non-tRNA regions within 5kb of tRNA genes

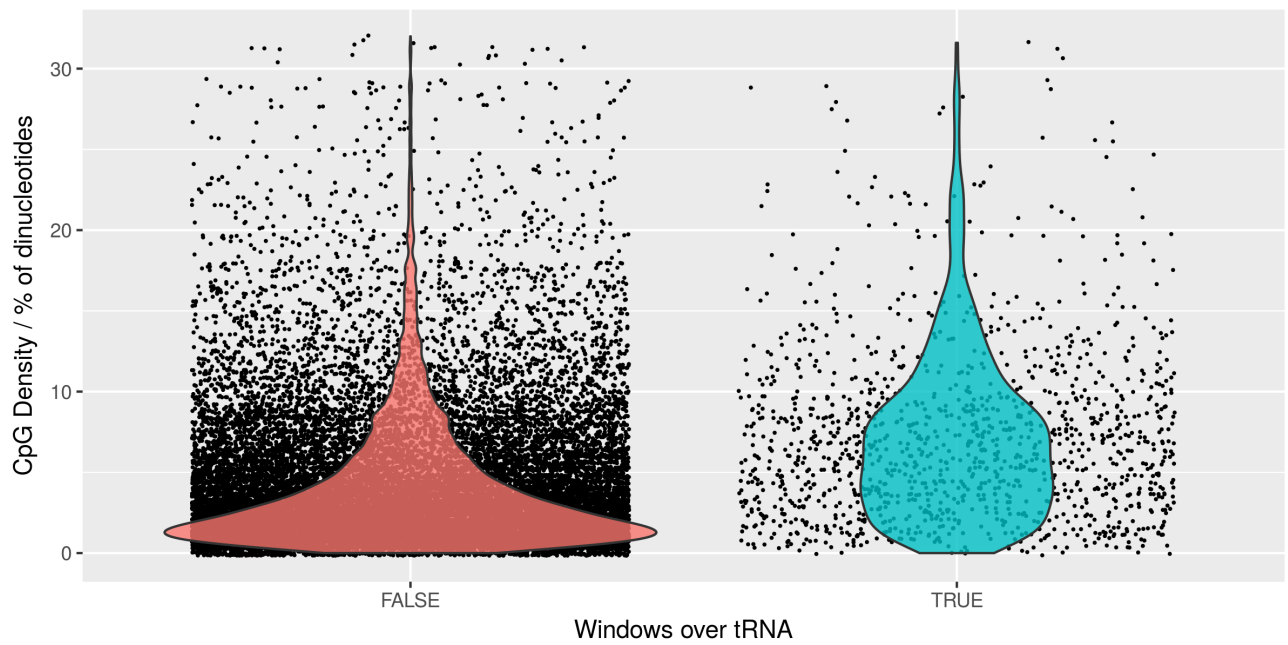


**Fig S8.** CpG Density in windows overlapping tRNA genes compared to that of non-tRNA overlapping windows in flanking sequences (+/-5kb)

## tRNA gene cluster numbers by bin size

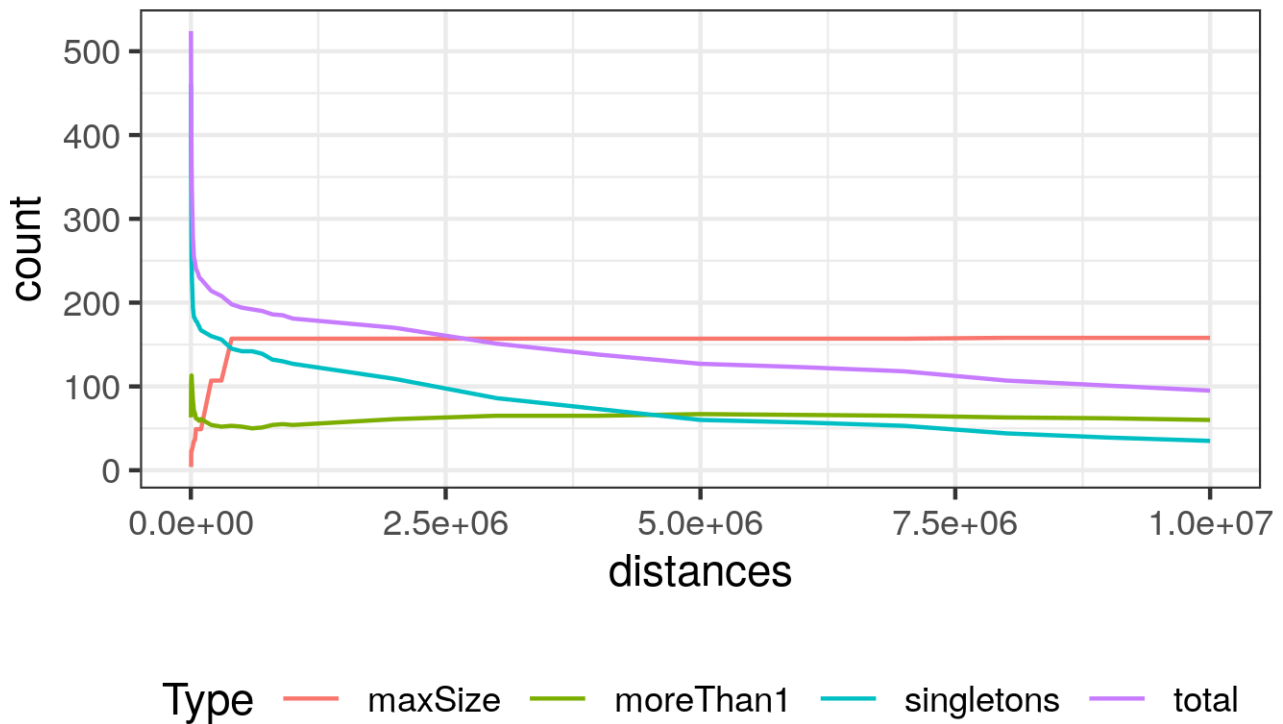


**Fig S9. tRNA gene cluster numbers at different bin sizes** total: total number of tRNA clusters.  
singletons: number of tRNAs in clusters alone. moreThan1: number of tRNAs in clusters with more than one tRNA. maxSize: the number of tRNAs in the largest cluster.